viral receptor clustering, which lowers the efficiency of virus-cell membrane fusion and thus affects viral replication.[4,43–45] In contrast, the Rac1-PAK pathway has been shown to support virus-cell membrane fusion.[46,47] Both processes require active actin reorganization.[4,42,44–47] Interestingly, HIV-1 Env-guided entry is supported by a Filamin A-RhoA-ROCK axis and Arp2/3 complex, both of which are commonly involved in actin cytoskeletal reorganization.[21,44] Our data link the reported functions of RhoA, Rac1, and RhoGDIs with the biological phenotype of ARHGDIB; inhibition of HIV-1 replication in T cells. This HIV-1 inhibitory function of ARHGDIB is exerted via simultaneous functional restriction of two Rho GTPases, RhoA and Rac1. It is likely that receptor clustering and virus-cell membrane fusion are affected in T cells ectopically overexpressing ARHGDIB. As receptor clustering is the initial event of the HIV-1 life cycle, HIV-1 replication is attenuated in such cells regardless of the route of HIV-1 entry. Also, in T cells ectopically overexpressing ARHGDIB, RhoA and Rac1 are substantially inactivated. However, they are not inactivated completely. Thus, these cells are still able to support HIV-1 replication at certain levels, contributing to the delayed HIV-1 replication phenotype in cells ectopically overexpressing ARHGDIB.

Some reports suggest that RhoA inhibits LTR-mediated transcription.[43,48,49] If this is the case, increased ARHGDIB expression should enhance LTR-mediated transcription. In PM1/ARHGDIB cells, HIV-1 LTR-driven luciferase activity was slightly enhanced (Fig. 3B), which is consistent with previously reported findings. On the other hand, HIV-1 replication was repressed in T cells, suggesting that this transcriptional effect on viral replication is modest, if it occurs at all. It is also possible that the enhancement of the luciferase signal may be due to increased endocytic activity in PM1/ARHGDIB cells, since the DEAE-Dextran protocol was employed for transfection, and similar levels of enhancement of CMV-driven transcription were observed in PM1/ARHGDIB cells as well.

Infection with VSV-G-pseudotyped HIV-1 and MLV, which enter cells via endocytosis accompanied by the rearrangement of actin filaments, is augmented in PM1/ARHGDIB cells (Fig. 3A). These findings are consistent with a previous report demonstrating that ARHGDIB stimulates endocytosis in cells with a lymphoid background.[50] The efficiency of VSV-G-pseudotyped MLV infection into PM1/ARHGDIB cells was higher than VSV-G-pseudotyped HIV-1. During the entry phase, HIV-1 utilizes microtubules to traffic toward the nucleus, whereas MLV does not seem to actively do so.[51,52] As ARHGDIB potentially inhibits Rho GTPases, thereby disturbing microtubular organization, it is possible that HIV-1 infection is blocked by ARHGDIB at the microtubule-dependent transport phase in addition to the receptor clustering phase. Alternatively, the relatively high infectious titers produced by the MLV vector may be responsible for the observed phenotype.

Our findings do not negate the possibility that ARHGDIB limits HIV-1 replication by restricting the functions of other effector molecules. For instance, ARHGDIB has also been shown to bind the RhoGEF protein Vav1 and the cytoskeletal protein ezrin, both of which have been implicated in the positive regulation of HIV-1 replication.[53–57] Thus, these factors may also contribute to the ARHGDIB-mediated inhibition of HIV-1 replication.

The treatment efficacy of HIV-1/AIDS by antiretroviral drugs has greatly improved. However, the adverse effects of antiretroviral drugs lower the quality of life of HIV-1-infected individuals, and the emergence of drug-resistant strains is anticipated for all of the currently available antiretroviral drugs. Insights into HIV-1-host interaction, such as that provided in this study, will aid in the design of novel antiretroviral drugs. Our findings may contribute not only to antiretroviral drug development but also to our understanding of viral pathogenesis. Considering the observation that a modest increase in ARHGDIB expression resulted in the inhibition of HIV-1 replication, it is possible that, at the later phase of HIV-1 infection, CD4-positive cells bearing higher levels of ARHGDIB may be selected. Thus, ARHGDIB levels may be useful as a progression marker of HIV-1 infection. HIV-1 disease progression may be delayed in individuals who have relatively high levels of ARHGDIB in CD4-positive T cells. These possibilities should be examined in future studies.

Acknowledgments

This work was supported in part by the Japan Human Science Foundation, the Japanese Ministry of Health, Labor and Welfare (Research on HIV/AIDS), and the Japanese Ministry of Education, Culture, Sports, Science and Technology (Priority Areas "Matrix of Infection Phenomena" 18073008).

Author Disclosure Statement

No competing financial interests exist.

References

1. Lu X, Wu X, Plemenitas A, *et al.*: CDC42 and Rac1 are implicated in the activation of the Nef-associated kinase and replication of HIV-1. Curr Biol 1996;6(12):1677–1684.
2. Cook JA, Albacker L, August A, and Henderson AJ: CD28-dependent HIV-1 transcription is associated with Vav, Rac, and NF-kappa B activation. J Biol Chem 2003;278(37):35812–35818.
3. Akasaki T, Koga H, and Sumimoto H: Phosphoinositide 3-kinase-dependent and -independent activation of the small GTPase Rac2 in human neutrophils. J Biol Chem 1999; 274(25):18055–18059.
4. del Real G, Jimenez-Baranda S, Mira E, *et al.*: Statins inhibit HIV-1 infection by down-regulating Rho activity. J Exp Med 2004;200(4):541–547.
5. Loomis RJ, Holmes DA, Elms A, Solski PA, Der CJ, and Su L: Citron kinase, a RhoA effector, enhances HIV-1 virion production by modulating exocytosis. Traffic 2006;7(12):1643–1653.
6. Pontow S, Harmon B, Campbell N, and Ratner L: Antiviral activity of a Rac GEF inhibitor characterized with a sensitive HIV/SIV fusion assay. Virology 2007;368(1):1–6.
7. Galandrini R, Henning SW, and Cantrell DA: Different functions of the GTPase Rho in prothymocytes and late pre-T cells. Immunity 1997;7(1):163–174.
8. Brown A, Wang X, Sawai E, and Cheng-Mayer C: Activation of the PAK-related kinase by human immunodeficiency virus type 1 Nef in primary human peripheral blood lymphocytes and macrophages leads to phosphorylation of a PIX-p95 complex. J Virol 1999;73(12):9899–9907.

9. Zhang B, Zhang Y, Dagher MC, and Shacter E: Rho GDP dissociation inhibitor protects cancer cells against drug-induced apoptosis. Cancer Res 2005;65(14):6054–6062.
10. Kolesnitchenko V, King L, Riva A, Tani Y, Korsmeyer SJ, and Cohen DI: A major human immunodeficiency virus type 1-initiated killing pathway distinct from apoptosis. J Virol 1997;71(12):9753–9763.
11. DerMardirossian C and Bokoch GM: GDIs: Central regulatory molecules in Rho GTPase activation. Trends Cell Biol 2005;15(7):356–363.
12. Dovas A and Couchman JR: RhoGDI: Multiple functions in the regulation of Rho family GTPase activities. Biochem J 2005;390(Pt 1):1–9.
13. Heasman SJ and Ridley AJ: Mammalian Rho GTPases: New insights into their functions from in vivo studies. Nat Rev Mol Cell Biol 2008;9(9):690–701.
14. Ladwein M and Rottner K: On the Rho'd: The regulation of membrane protrusions by Rho-GTPases. FEBS Lett 2008;582(14):2066–2074.
15. Brass AL, Dykxhoorn DM, Benita Y, *et al.*: Identification of host proteins required for HIV infection through a functional genomic screen. Science 2008;319(5865):921–926.
16. Zhou H, Xu M, Huang Q, *et al.*: Genome-scale RNAi screen for host factors required for HIV replication. Cell Host Microbe 2008;4(5):495–504.
17. Simmons A, Gangadharan B, Hodges A, *et al.*: Nef-mediated lipid raft exclusion of UbcH7 inhibits Cbl activity in T cells to positively regulate signaling. Immunity 2005;23(6):621–634.
18. Hodges A, Sharrocks K, Edelmann M, *et al.*: Activation of the lectin DC-SIGN induces an immature dendritic cell phenotype triggering Rho-GTPase activity required for HIV-1 replication. Nat Immunol 2007;8(6):569–577.
19. Urano E, Ichikawa R, Morikawa Y, Yoshida T, Koyanagi Y, and Komano J: T cell-based functional cDNA library screening identified SEC14-like 1a carboxy-terminal domain as a negative regulator of human immunodeficiency virus replication. Vaccine 2010;28(Suppl 2):B68–B74.
20. Urano E, Kariya Y, Futahashi Y, *et al.*: Identification of the P-TEFb complex-interacting domain of Brd4 as an inhibitor of HIV-1 replication by functional cDNA library screening in MT-4 cells. FEBS Lett 2008;582(29):4053–4058.
21. Komano J, Miyauchi K, Matsuda Z, and Yamamoto N: Inhibiting the Arp2/3 complex limits infection of both intracellular mature vaccinia virus and primate lentiviruses. Mol Biol Cell 2004;15(12):5197–5207.
22. Kimura K, Tsuji T, Takada Y, Miki T, and Narumiya S: Accumulation of GTP-bound RhoA during cytokinesis and a critical role of ECT2 in this accumulation. J Biol Chem 2000;275(23):17233–17236.
23. Takahashi Y, Tanaka Y, Yamashita A, Koyanagi Y, Nakamura M, and Yamamoto N: OX40 stimulation by gp34/OX40 ligand enhances productive human immunodeficiency virus type 1 infection. J Virol 2001;75(15):6748–6757.
24. Vicente-Manzanares M, Viton M, and Sanchez-Madrid F: Measurement of the levels of polymerized actin (F-actin) in chemokine-stimulated lymphocytes and GFP-coupled cDNA transfected lymphoid cells by flow cytometry. Methods Mol Biol 2004;239:53–68.
25. Shimizu S, Urano E, Futahashi Y, *et al.*: Inhibiting lentiviral replication by HEXIM1, a cellular negative regulator of the CDK9/cyclin T complex. AIDS 2007;21(5):575–582.
26. Sato K, Aoki J, Misawa N, *et al.*: Modulation of human immunodeficiency virus type 1 infectivity through incorporation of tetraspanin proteins. J Virol 2008;82(2):1021–1033.
27. Togawa A, Miyoshi J, Ishizaki H, *et al.*: Progressive impairment of kidneys and reproductive organs in mice lacking Rho GDIalpha. Oncogene 1999;18(39):5373–5380.
28. Reif K and Cantrell DA: Networking Rho family GTPases in lymphocytes. Immunity 1998;8(4):395–401.
29. Tuosto L, Michel F, and Acuto O: p95vav associates with tyrosine-phosphorylated SLP-76 in antigen-stimulated T cells. J Exp Med 1996;184(3):1161–1166.
30. Stowers L, Yelon D, Berg LJ, and Chant J: Regulation of the polarization of T cells toward antigen-presenting cells by Ras-related GTPase CDC42. Proc Natl Acad Sci USA 1995;92(11):5027–5031.
31. Boulter E, Garcia-Mata R, Guilluy C, *et al.*: Regulation of Rho GTPase crosstalk, degradation and activity by RhoGDI1. Nat Cell Biol 2010;12(5):477–483.
32. Etienne-Manneville S and Hall A: Rho GTPases in cell biology. Nature 2002;420(6916):629–635.
33. Dransart E, Morin A, Cherfils J, and Olofsson B: RhoGDI-3, a promising system to investigate the regulatory function of rhoGDIs: uncoupling of inhibitory and shuttling functions of rhoGDIs. Biochem Soc Trans 2005;33(Pt 4):623–626.
34. Lee SH and Dominguez R: Regulation of actin cytoskeleton dynamics in cells. Mol Cells 2010;29(4):311–325.
35. Takaishi K, Kikuchi A, Kuroda S, Kotani K, Sasaki T, and Takai Y: Involvement of rho p21 and its inhibitory GDP/GTP exchange protein (rho GDI) in cell motility. Mol Cell Biol 1993;13(1):72–79.
36. Miura Y, Kikuchi A, Musha T, *et al.*: Regulation of morphology by rho p21 and its inhibitory GDP/GTP exchange protein (rho GDI) in Swiss 3T3 cells. J Biol Chem 1993;268(1):510–515.
37. Komuro R, Sasaki T, Takaishi K, Orita S, and Takai Y: Involvement of Rho and Rac small G proteins and Rho GDI in Ca2+-dependent exocytosis from PC12 cells. Genes Cells 1996;1(10):943–951.
38. Laguette N, Sobhian B, Casartelli N, *et al.*: SAMHD1 is the dendritic- and myeloid-cell-specific HIV-1 restriction factor counteracted by Vpx. Retrovirology 2011;474(7353):654–657.
39. Koning FA, Newman EN, Kim EY, Kunstman KJ, Wolinsky SM, and Malim MH: Defining APOBEC3 expression patterns in human tissues and hematopoietic cell subsets. J Virol 2009;83(18):9474–9485.
40. Refsland EW, Stenglein MD, Shindo K, Albin JS, Brown WL, and Harris RS: Quantitative profiling of the full APOBEC3 mRNA repertoire in lymphocytes and tissues: Implications for HIV-1 restriction. Nucleic Acids Res 2010;38(13):4274–4284.
41. Ridley AJ: Rho GTPases and cell migration. J Cell Sci 2001;114(Pt 15):2713–2722.
42. Fukata M, Nakagawa M, and Kaibuchi K: Roles of Rho-family GTPases in cell polarisation and directional migration. Curr Opin Cell Biol 2003;15(5):590–597.
43. Iyengar S, Hildreth JE, and Schwartz DH: Actin-dependent receptor colocalization required for human immunodeficiency virus entry into host cells. J Virol 1998;72(6):5251–5255.
44. Jimenez-Baranda S, Gomez-Mouton C, Rojas A, *et al.*: Filamin-A regulates actin-dependent clustering of HIV receptors. Nat Cell Biol 2007;9(7):838–846.
45. Malinowsky K, Luksza J, and Dittmar MT: Susceptibility to virus-cell fusion at the plasma membrane is reduced through expression of HIV gp41 cytoplasmic domains. Virology 2008;376(1):69–78.
46. Pontow SE, Heyden NV, Wei S, and Ratner L: Actin cytoskeletal reorganizations and coreceptor-mediated activation

of rac during human immunodeficiency virus-induced cell fusion. J Virol 2004;78(13):7138–7147.
47. Harmon B and Ratner L: Induction of the Galpha(q) signaling cascade by the human immunodeficiency virus envelope is required for virus entry. J Virol 2008;82(18):9191–9205.
48. Wang L, Zhang H, Solski PA, Hart MJ, Der CJ, and Su L: Modulation of HIV-1 replication by a novel RhoA effector activity. J Immunol 2000;164(10):5369–5374.
49. Helms WS, Jeffrey JL, Holmes DA, Townsend MB, Clipstone NA, and Su L: Modulation of NFAT-dependent gene expression by the RhoA signaling pathway in T cells. J Leukoc Biol 2007;82(2):361–369.
50. Lamaze C, Chuang TH, Terlecky LJ, Bokoch GM, and Schmid SL: Regulation of receptor-mediated endocytosis by Rho and Rac. Nature 1996;382(6587):177–179.
51. Sodeik B: Unchain my heart, baby let me go—the entry and intracellular transport of HIV. J Cell Biol 2002;159(3):393–395.
52. Naghavi MH and Goff SP: Retroviral proteins that interact with the host cell cytoskeleton. Curr Opin Immunol 2007;19(4):402–407.
53. Haedicke J, de Los Santos K, Goff SP, and Naghavi MH: The Ezrin-radixin-moesin family member ezrin regulates stable microtubule formation and retroviral infection. J Virol 2008;82(9):4665–4670.
54. Hecker C, Weise C, Schneider-Schaulies J, Holmes HC, and ter Meulen V: Specific binding of HIV-1 envelope protein gp120 to the structural membrane proteins ezrin and moesin. Virus Res 1997;49(2):215–223.
55. Kubo Y, Yoshii H, Kamiyama H, *et al.*: Ezrin, Radixin, and Moesin (ERM) proteins function as pleiotropic regulators of human immunodeficiency virus type 1 infection. Virology 2008;375(1):130–140.
56. Barrero-Villar M, Cabrero JR, Gordon-Alonso M, *et al.*: Moesin is required for HIV-1-induced CD4-CXCR4 interaction, F-actin redistribution, membrane fusion and viral infection in lymphocytes. J Cell Sci 2009;122(Pt 1):103–113.
57. Fackler OT, Luo W, Geyer M, Alberts AS, and Peterlin BM: Activation of Vav by Nef induces cytoskeletal rearrangements and downstream effector functions. Mol Cell 1999; 3(6):729–739.

Address correspondence to:
Jun Komano
AIDS Research Center
National Institute of Infectious Diseases
1-23-1 Toyama, Shinjuku
Tokyo 162-8640, Japan

E-mail: ajkomano@nih.go.jp

Gene Therapy (2011) 18, 936–941

www.nature.com/gt

SHORT COMMUNICATION

Protein transduction by pseudotyped lentivirus-like nanoparticles

T Aoki[1,2], K Miyauchi[1,2], E Urano[1], R Ichikawa[1] and J Komano[1]

A simple, efficient and reproducible method to transduce proteins into mammalian cells has not been established. Here we describe a novel protein transduction method based on a lentiviral vector. We have developed a method to package several thousand foreign protein molecules into a lentivirus-like nanoparticle (LENA) and deliver them into mammalian cells. In this proof-of-concept study, we used β-lactamase (BlaM) as a reporter molecule. The amino-terminus of BlaM was fused to the myristoylation signal of *lyn*, which was placed upstream of the amino-terminus of *Gag* (BlaM-gag-pol). By co-transfection of plasmids encoding BlaM-gag-pol and vesicular stomatitis virus-G (VSV-G) into 293T cells, LENA were produced containing BlaM enzyme molecules as many as Gag per capsid, which has been reported to be ~5000 molecules, but lacking the viral genome. Infection of 293T and MT-4 cells by VSV-G-pseudotyped BlaM-containing LENA led to successful transduction of BlaM molecules into the cell cytoplasm, as detected by cleavage of the fluorescent BlaM substrate CCF2-AM. LENA-mediated transient protein transduction does not damage cellular DNA, and the preparation of highly purified protein is not necessary. This technology is potentially useful in various basic and clinical applications.
Gene Therapy (2011) **18,** 936–941; doi:10.1038/gt.2011.38; published online 31 March 2011

Keywords: LENA; BlaM; Gag; protein transduction; lentiviral vector

INTRODUCTION

When viruses infect cells the viral contents are released. A virus can, therefore, be considered as a protein transduction vehicle into a target cell if a large number of foreign proteins are packaged per virion. A lentiviral vector, approved for human gene therapy,[1] has been produced by transfecting 293T cells with four plasmids: the gene transfer vector that provides the viral genome packaged into the virion, and three plasmid vectors, each expressing *gag–pol*, *rev* or the vesicular stomatitis virus-G (VSV-G) genome.[2–4] The *gag–pol* expression vector produces Gag and Gag-pol in a ratio of ~20:1 because of the frameshift signal positioned between the *gag* and *pol* open reading frames.[5] Gag ($Pr55^{Gag}$) is a viral structural protein that traffics to the plasma membrane aided by its amino-terminal myristoyl group, and self-oligomerizes at the plasma membrane to form a spherical structure.[6] The expression of Gag alone leads to the production of an enveloped virus-like particle (VLP) of ~100 nm in diameter, consisting of ~5000 Gag molecules.[7]

When the *gag–pol* expression vector is used to produce VLP, both Gag and Gag-pol proteins, a total of 5000 molecules,[7] form the lentiviral nanoparticles in which approximately one-twentieth of the VLP-forming protein is Gag-pol.[5] The VLP produced by the *gag–pol* expression vector undergoes maturation whereby Gag is processed by the protease made from Pol. Gag is cleaved into $p17^{MA}$, $p24^{CA}$ and other smaller fragments. This changes the shape of the VLP core from doughnut shape to bullet shape, as visualized by electron microscopy. Mediated by VSV-G, the mature VLP envelope fuses to the cell membrane more efficiently than the immature VLP.[8] In accordance with this process, if a foreign protein is fused to lentiviral Gag, a large number of foreign proteins should be transduced into mammalian cells. In this work, the lentiviral vector has been engineered to achieve this goal.

By co-transfecting two plasmid vectors, each expressing *gag–pol* or VSV-G, the lentivirus-like nanoparticles (LENA) can be produced with a VSV-G envelope (Figure 1a). These particles undergo maturation, and should be highly competent for promoting fusion of LENA envelope to the cell membrane. The VSV-G-pseudotyped LENA should be capable of releasing viral content into the target cells. We have named this process 'pseudoinfection' because it mimics viral infection, but is not accompanied by integration of the viral genome into chromosomal DNA.

We have previously shown that substitution of the human immunodeficiency virus type 1 (HIV-1) Gag myristoylation signal with the phospholipase C-δ 1 pleckstrin homology (PH) domain, or attachment of heterologous myristoylation signals to the amino-terminus of Gag, increases the production of lentiviral vector.[9,10] In these studies we used the human codon-optimized *gag–pol* to maximize viral protein synthesis. The infectivity of these pseudovirions was comparable with that of the wild-type (WT) counterpart. This is noteworthy because modification of Gag often results in reduction of viral productivity and infectivity.[11,12] It has been reported recently that a protein transduction using murine leukemia virus is achievable by embedding a foreign gene in *gag*. However, the viral productivity and infectivity need to be improved by WT Gag-pol provided in *trans* upon viral production. These data suggest that by fusing a foreign protein to the amino-terminus of Gag and providing a membrane-targeting signal, it is possible to produce a high-titer, uniform, foreign protein-containing LENA without the need to co-transfect the WT Gag-pol expression plasmid. We tested whether the VSV-G-pseudotyped

[1]AIDS Research Center, National Institute of Infectious Diseases, Shinjuku-ku, Tokyo, Japan
Correspondence: Dr J Komano, AIDS Research Center, National Institute of Infectious Diseases, Toyama, 1-23-1, Shinjuku-ku, Tokyo 162-8640, Japan.
E-mail: ajkomano@nih.go.jp
[2]These authors contributed equally to this work.
Received 29 August 2010; revised 2 December 2010; accepted 3 January 2011; published online 31 March 2011

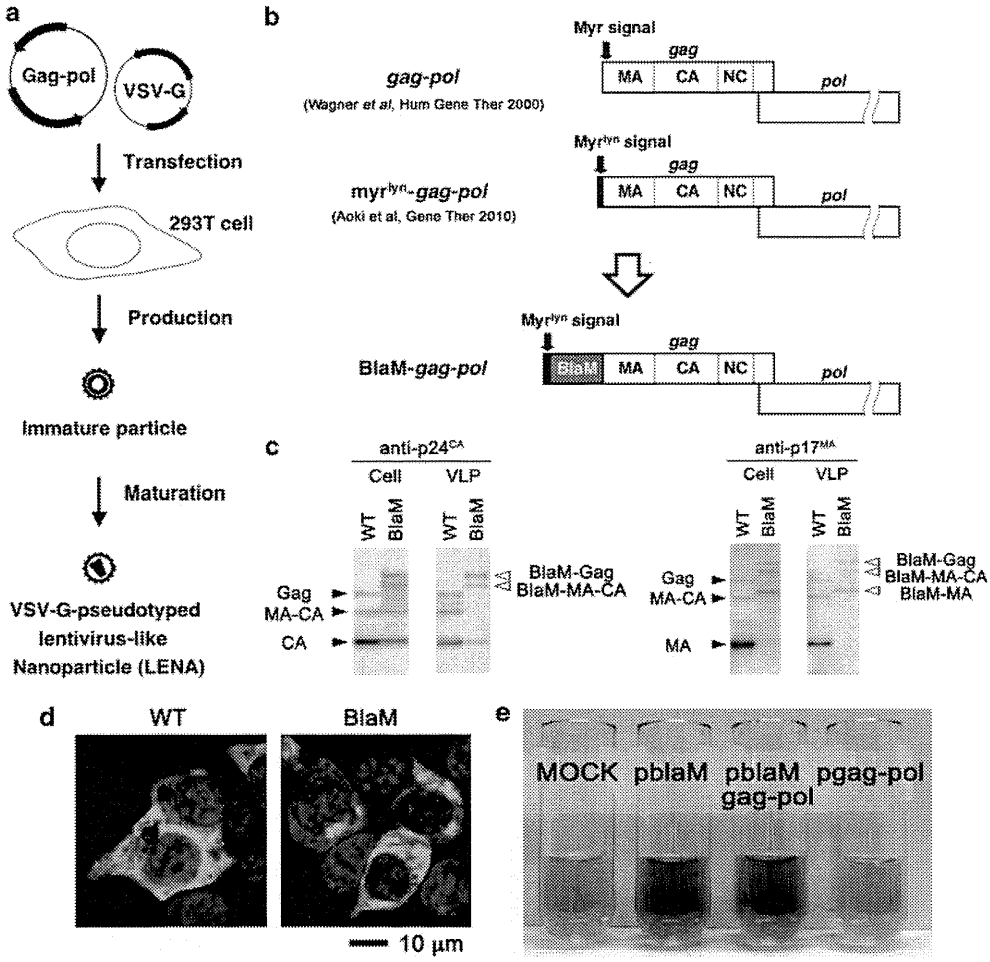

Figure 1 Production of a BlaM-containing LENA pseudotyped with VSV-G. (**a**) Schematic representation of production of VSV-G-pseudotyped LENA. Two plasmids are transfected into 293T cells, and LENA is recovered from the culture supernatant at 48 h post-transfection. The viral protease is activated after the VLP is released from the cell, and it mediates the maturation of the particles. (**b**) The structure of WT *gag–pol*, a mutant bearing the myristoylation signal of *lyn* (myr^{lyn}*-gag-pol*), and *blaM-gag-pol*. Gag is cleaved into p17^{MA} (MA), p24^{CA} (CA), nucleocapsid (NC) and other domains by the viral protease encoded in *pol*. In the myr^{lyn}*-gag-pol* and *blaM-gag-pol* constructs, the Gag translational initiation site and the myristoylation target residues were mutated to leucine and alanine to minimize internal translational initiation and myristoylation. (**c**) Verification of protein expression and VLP production of BlaM-gag-pol construct in 293T cells by western blot analysis using anti-p24^{CA} and anti-p17^{MA} antibodies. Shown are the analyses of cell lysates (Cell) transfected with p*gag-pol* (WT) or p*blaM-gag-pol* (BlaM), and the viral particles (VLP) collected from the culture supernatant of transfected cells. Pr55^{Gag} (~55 kDa, Gag), the Gag proteolytic cleavage intermediate MA–CA (~40 kDa) and the complete proteolytic cleavage product p24^{CA} (~24 kDa, CA) and p17^{MA} (~17 kDa, MA) are indicated by arrowheads. BlaM-Gag, BlaM-MA-CA and BlaM-MA have higher molecular weights because of the attachment of BlaM (~30 kDa) to the MA domain. (**d**) Immunofluorescence assay showing the distribution of WT Gag (WT) or BlaM-Gag (BlaM) in 293T cells transfected with p*gag-pol* or p*blaM-gag-pol*. Green and blue represent the anti-p24^{CA} monoclonal antibody-stained signal and the Hoechst 33258-stained nucleus, respectively. Magnification ×400; scale bar, 10 μm. (**e**) BlaM enzyme activity was tested by nitrocefin. Lysates from 293T cells transfected with p*blaM*, p*blaM-gag-pol*, *or* p*gag-pol* or untransfected cells (MOCK) were incubated with nitrocefin for 30 min at 37 °C.

LENA could serve as a protein transduction vehicle for mammalian cells using β-lactamase (BlaM) as a reporter.

RESULTS AND DISCUSSION

BlaM was chosen as reporter molecule because mammalian cells do not have BlaM activity. Also, a cell-membrane-permeable BlaM substrate is available, which can distinguish LENA content release from cellular endocytosis of LENA that can occur without membrane fusion.[13] *BlaM* was fused to the amino-terminus of *gag–pol*, and the *lyn* myristoylation signal was attached to the amino-terminus of *BlaM* (*BlaM-gag-pol*; Figure 1b). The codon usage of *gag–pol* has been human codon optimized, but bearing the natural −1 frameshift signal at the *gag–pol* junction.[14] Thus, the vector provides the natural Gag to Gag-pol ratio. The BlaM-gag-pol protein was produced in 293T cells as expected (Figure 1c). The *BlaM* construct produced VLP from the transfected cells, although the efficiency was less than with WT *gag–pol* (Figure 1c). The processing efficacy of Gag in BlaM VLP was less efficient compared with the WT as highlighted by the absence of free matrix domain (MA) signal in BlaM VLP, which was because of the lack of HIV-1 protease recognition motif between BlaM and MA (right panel, Figure 1c). In 293T cells transiently transfected with this plasmid, the BlaM-gag-pol fusion protein distribution was similar to that of the WT, although with some aggregation in the cytoplasm (Figure 1d). The BlaM-gag-pol fusion protein retained enzyme activity as demonstrated by its reaction with the BlaM substrate nitrocefin, which changed from a straw color to brown when incubated with

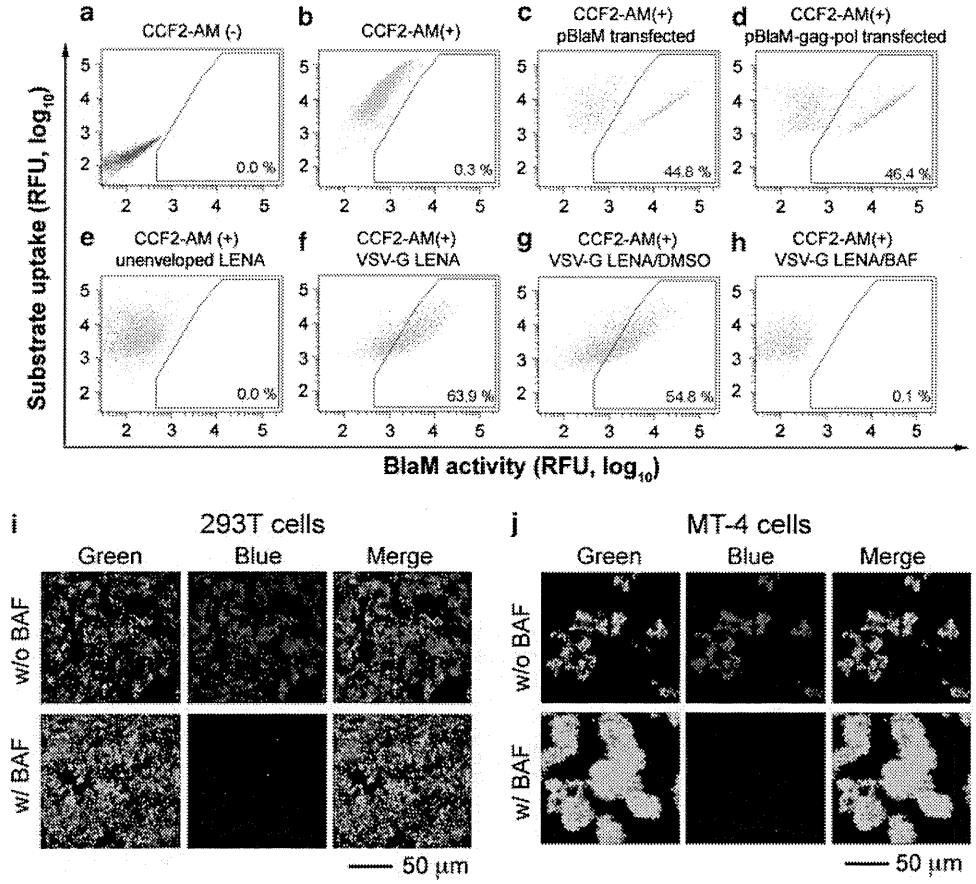

Figure 2 Flow cytometric analysis to measure the BlaM transduction into 293T cells by VSV-G-pseudotyped BlaM-LENA. The 293T cells were grown in 24-well plates and either transfected or pseudoinfected with LENA preparations. (**a**) Unstained 293T cells. (**b**) 293T cells loaded with CCF2-AM. (**c**, **d**) 293T cells were transfected with pBlaM (**c**) or pBlaM-gag-pol (**d**), and loaded with CCF2-AM at 48 h post-transfection before the flow cytometric analysis. (**e**–**h**) 293T cells were exposed to unenveloped BlaM-LENA (**e**) or VSV-G-pseudotyped BlaM-LENA (**f**–**h**). Cells were loaded with CCF2-AM at 2 h post-LENA exposure. (**g**, **h**) The VSV-G-dependent BlaM transduction was verified by exposing 293T cells with VSV-G-pseudotyped BlaM-LENA in the presence of bafilomycin A1 (BAF) at a concentration of 10 μg ml^{-1} (**h**). Dimethylsulfoxide (DMSO) was used as a control (**g**). The percentage of the gated population is noted in each panel. The *x* axis represents the blue fluorescence, reflecting the BlaM activity (relative fluorescent unit (RFU)). The *y* axis represents the green fluorescence, reflecting the substrate loading onto the cells. (**i**, **j**) Microscopic detection of BlaM transduction in 293T cells (**i**) or MT-4 cells (**j**) by VSV-G-pseudotyped BlaM-LENA. Cells were exposed to BlaM-LENA for 3 h, and loaded with CCF2-AM overnight at room temperature in the presence (10 μg ml^{-1}) or absence of BAF (w/BAF or w/o BAF, respectively). The bar represents 50 μm, magnification ×200.

lysates from 293T cells transfected with the BlaM-gag-pol expression vector (Figure 1e). The BlaM enzyme activity of BlaM-gag-pol was indistinguishable from that of WT BlaM (Figure 1e). BlaM enzyme activity was not detected in MOCK or p*gag-pol*-transfected cell lysates (Figure 1e).

Protein transduction into 293T cells was conducted by exposing target cells to VSV-G-pseudotyped BlaM-LENA, which mimics viral infection. The success of BlaM transduction into the target cell cytoplasm was judged by using the cytoplasm-retained BlaM substrate, CCF2-AM, which yields blue fluorescence upon cleavage by BlaM enzyme activity.

The 293T cells emitted green fluorescence when they were loaded with CCF2-AM (Figure 2, compare a vs b). When 293T cells were transfected with expression vectors for BlaM or the BlaM-gag-pol, substrate cleavage, as demonstrated by a shift to blue fluorescence, was detected in a discrete population of cells, representing a transfection efficiency of ~45% (Figures 2c and d). These data suggest that transduced BlaM-gag-pol has BlaM activity, consistent with the results of the nitrocefin assay (Figure 1e). When BlaM was transduced into 293T cells by VSV-G-pseudotyped BlaM-LENA, a significant shift from green to blue fluorescence was detected (63.9%, Figure 2f). The rightward shift of the signal along the *x* axis suggests that almost all the cells were transduced with BlaM by BlaM-LENA. BlaM transduction was dependent on VSV-G function as CCF2-AM cleavage was not detected by LENA lacking VSV-G (Figure 2e), and BlaM transduction was inhibited by bafilomycin A1 that blocks VSV-G-mediated membrane fusion (Figure 2, compare g vs h). The catalytic activity was visualized under the fluorescent microscopy. In agreement with the flow cytometric analysis, almost all the substrate-loaded 293T cells exposed to BlaM-LENA became blue fluorescent in experimental conditions comparable with the above experiments, and the catalytic activity was not detected when cells were treated with bafilomycin A1 (Figure 2i). The blue fluorescence was detected homogenously in the cell cytoplasm (Figure 2i). These data were reproduced in human T-cell line MT-4 (Figure 2j). Considering the critical dependence to VSV-G, it is highly unlikely that the BlaM activity was derived from the residual DNA/lipid mixture in the LENA preparation. The BlaM-transducing unit into 293T cells was $\sim 0.8 \pm 0.01 \times 10^9$ ml^{-1} as

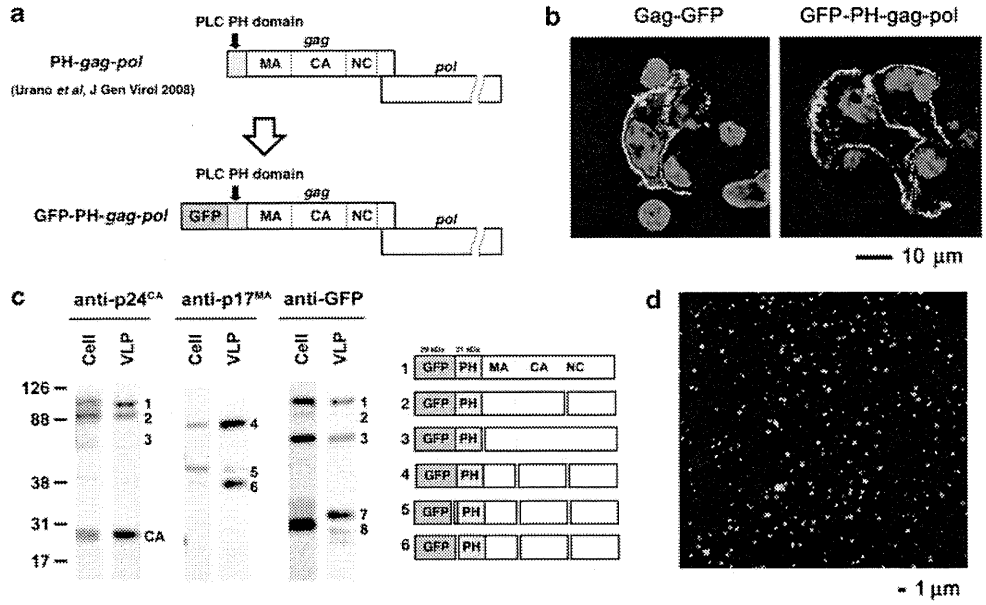

Figure 3 Production of a GFP-containing lentivirus-like nanoparticle for physical counting. (**a**) The structure of PH-*gag-pol* and GFP-PH-*gag-pol*. (**b**) The distribution of Gag-GFP and GFP-PH-gag-pol in transiently transfected 293T cells examined by confocal microscopy. The images were taken at 24 h post-transfection. The bar represents 10 μm, magnification ×630. (**c**) Verification of protein expression and VLP production of GFP-PH-gag-pol construct in 293T cells by western blot analysis using anti-$p24^{CA}$, anti-$p17^{MA}$ and anti-GFP antibodies. Shown are the analyses of cell lysates (Cell) transfected with pGFP-PH-*gag-pol* and the viral particles (VLP) collected from the culture supernatant of transfected cells. The numbers represent the proteolytic products as illustrated in the right panel estimated from the western blot analysis. (**d**) Confocal image of the GFP-PH-LENA on the slide glass. The bar represents 1 μm, magnification ×630.

estimated by the BlaM-LENA serial dilution (data not shown). Thus, 293T cells were exposed to ~1000-fold excess of BlaM-LENA.

We constructed GFP-PH-LENA to visualize the LENA particles (Figure 3a). In this construct, the PH domain from phospholipase C-δ 1 functions as the membrane targeting motif.[9,10] The GFP-PH-gag-pol was distributed at cell periphery, similar to Gag-GFP (Figure 3b). The VLP production by GFP-PH-gag-pol was verified in western blot analysis (Figure 3c). According to the estimated molecular weight of protease-mediated cleavage products, we speculate the possible protease recognition sites within green fluorescent protein (GFP), GFP–PH junction and PH–MA junction, although we did not intentionally reconstitute the HIV-1 protease recognition sites in these positions (Figure 3c). The GFP-encapsidated LENA preparations were spotted onto the poly-L-lysine-coated slide glass, and the captured LENA was imaged by the confocal microscopy. By counting the green fluorescent dot signals per unit area, we estimated the number of GFP-PH-LENA particles as $1.4 \pm 0.2 \times 10^9\ ml^{-1}$ (Figure 3d), which was similar to the BlaM-transduction unit of VSV-G-pseudotyped BlaM-LENA.

To test whether the lentivirus vector used to produce BlaM-LENA retained any viral infectivity, a lentivirus vector was produced carrying the luciferase gene, using the four plasmid system[9,10] with the BlaM-gag-pol construct, and then viral infectivity was assessed. Gene transduction by this lentiviral vector was undetectable. These data indicate that transfer to target cells by BlaM-LENA of an expressed, endogenous retroviral element from 293T cells is unlikely to occur. These data show that a protein transduction system based on LENA would have an extra level of safety compared with the protein transduction system based on a retroviral vector system.[11]

Protein transduction in a broad sense, referring to the transport of protein across the cell membrane, is a useful technique in experimental molecular biology. It does not require *de novo* transcription and translation, and the transferred protein functions immediately after the transduction. Proteins, however, do not easily pass through the plasma membrane. Historically, microinjection, electroporation and cell-permeable peptide motifs were used to introduce proteins into cells.[15–17] These methods, however, demand a highly purified protein, technical skill or specialized, costly equipment. Also, variable results have been obtained using different proteins and target cells. The need of a highly purified protein applies to protein lipofection to yield the reproducible results. A convenient, fast, highly efficient and reproducible protein transduction method has so far remained undeveloped. Such a technique would greatly help the generation of safe, induced pluripotent stem cells. LENA production is as straightforward as co-transfecting two plasmids into 293T cells without *trans*-complementing the WT *gag–pol* expression vector, and furthermore the therapeutic protein is protected from plasma proteases by a lipid bilayer. The target cell tropism can be controlled by well-established viral pseudotype techniques. Using LENA, a substantial number of protein molecules can be packaged into the nanoparticles, and the transduction procedure is as easy as exposing mammalian cells with LENA. There is no need to prepare highly purified proteins for the LENA system. Also, target proteins are post-translationally modified in human cells, which should be better than the protein modification in non-human organisms. It should also be possible to increase the amount of protein that can be delivered into cells by concentrating the LENA preparation. Physical counting of GFP-encapsidated LENA shows that a high-titer LENA preparation was casually produced. In this study, we did not introduce protease recognition sites into myristoylation signal-BlaM or -BlaM-MA junctions. By doing so, we would have possibly liberated the foreign protein from the precursor. This could result in infectious LENA particles as the free MA is in part important for the viral infectivity.[9]

Currently, few approaches are available for the incorporation of a foreign protein into retro- or lenti-viral VLP. The protein of interest

can be fused to the C-terminus of Gag or inserted into the middle of the Gag protein (for example, between the MA and CA).[11,12] Foreign protein fusion to the C-terminus of Gag would destroy the frameshift signal required to produce Gag-pol. Thus, Pol would no longer be produced. To maintain efficient pseudoinfection, the *gag–pol* expression vector must be provided in *trans* when the VLP is produced. The latter approach often results in reduced VLP yield. Thus, again, to increase the VLP yield, the *gag–pol* expression vector has to be co-transfected with the plasmid encoding Gag fused to the foreign protein. Co-transfection of the *gag–pol* expression vector is likely to reduce the amount of foreign protein per VLP, and lower its uniformity. It is, therefore, desirable not to co-transfect with the WT *gag–pol* expression plasmid. Alternatively, Vpr can be used to incorporate foreign proteins into lentiviral particles.[18] Only a few dozen protein molecules, however, are packed per particle, rendering this approach of little use in protein transduction. In summary, fusion of a foreign protein to the N-terminus of Gag has the advantages of producing uniform, high-titer and membrane fusion-competent VLP without *trans*-complementation by WT Gag-pol.

The disadvantages of the LENA system are the susceptibility of foreign proteins to viral protease and the restriction in the molecular sizes of foreign proteins. We have succeeded in generating Gag-LacZ VLP, suggesting that the production of LENA carrying a foreign protein with a molecular weight of ~100 kDa is feasible. The yield, however, of LENA gradually decreases as the molecular weight of the foreign protein increases. We did not detect proteolytic cleavage of BlaM by viral protease in LENA particles; however, when we tested the transcriptional regulator of HTLV-1 (human T-cell leukemia virus type 1), Tax, it was degraded by viral protease. To overcome these potential disadvantages, it is worth considering the use of only the minimal functional domain of a foreign protein and the destruction of potential protease recognition sites in the foreign protein without losing its function.

Lentiviral vectors have been approved for human gene therapy.[1] LENA does not contain a viral genome, and is unlikely to support the transfer of endogenous retrovirus-like elements; thus, the cellular genome is not threatened by LENA-mediated protein transduction. Thus, a major safety concern associated with retroviral or lentiviral vectors is alleviated, making LENA applicable for *in vivo* studies. Retroviral vectors are often used for induced pluripotent stem cell genesis.[19] However, they can damage the cellular genome, and transduced gene expression is difficult to shut off, which can lead to malignant transformation of induced pluripotent stem cells. To overcome this problem, a transient and efficient protein transduction method is needed. We believe that LENA addresses these issues. Altogether, our system has many advantages over currently available protein transduction protocols, suggesting that it should be considered for basic and clinical applications.

MATERIALS AND METHODS

Plasmids

The following oligonucleotides were annealed, and cloned into the *AfeI–AgeI* sites of pEGFP-C2 (Clontech, Palo Alto, CA, USA) to generate the p*lyn*MyEGFP-C2: 5′-GCTACCGGACTCAGATCTCGAGCTCAAGCTTCGAATTGC CACCATGGGATGTATTAAATCAAAAAGGAAAGACGATCCA-3′ and 5′-CCG GTGGATCGTCTTTCCTTTTTGATTTAATACATCCCATGGTGGCAATTCGA AGCTTGAGCTCGAGATCTGAGTCCGGTAGC-3′. The *SnaBI–EcoRI* fragment from p*lyn*MyEGFP-C2 was cloned into the corresponding sites of pPH-*gag-pol*,[9] generating p*lyn*MyGFP-*gag-pol*. The β-lactamase gene from pUC19 was amplified by the following primers: 5′-ACCGGTCAATCCAGAAACGCTGGTG AAAG-3′ and 5′-CAATTGCCAATGCTTAATCAGTGAGGC-3′. The *AgeI–MfeI* fragment of the PCR fragment was cloned into the *AgeI–EcoRI* sites of p*lyn*MyGFP-*gag-pol*, generating the p*blaM-gag-pol*. The expression vector for VSV-G was described previously.[20] The original codon-optimized HIV-1 *gag–pol* expression vector was described previously.[14] The Gag-GFP expression vector was described previously.[10] The pGFP-PH-*gag-pol* was constructed by inserting the *NdeI–PshAI* fragment from pEGFP-PLCd1 PH[21] into the corresponding sites of pPH-*gag-pol*.[9] pcDNA3 was obtained from Invitrogen (Tokyo, Japan).

Cells and transfection

The 293T cells, obtained from Invitrogen as 293FT cells (Invitrogen), were maintained in RPMI-1640 medium (Sigma, St Louis, MA, USA) supplemented with 10% fetal bovine serum (Japan Bioserum, Tokyo, Japan), 50 U ml^{-1} penicillin and 50 μg ml^{-1} streptomycin (Invitrogen), at 37 °C in a humidified 5% CO_2 atmosphere. Cells were transfected with DNA using Lipofectamine 2000 according to the manufacturer's protocol (Invitrogen), or calcium phosphate precipitation. To produce VSV-G-pseudotyped BlaM-LENA, equal amounts of pVSV-G and p*blaM-gag-pol* were transfected into 293T cells. Unenveloped BlaM-LENA was produced using pcDNA3 in place of pVSV-G.

Immunological detection

The detection of viral gene products by western blot analysis was performed as described previously,[22] except that the anti-p24^{CA} monoclonal antibody clone 183-H12-5C and the anti-p17^{MA} rabbit antiserum (NIH AIDS Research and Reference Reagent Program) were used. The immunofluorescent analysis was performed as described previously,[22] except that cells were fixed at 24 h post-transfection, and the following reagents were used: anti-p24^{CA} monoclonal antibody (clone 183-H12-5C), anti-mouse antibody conjugated with biotin (Invitrogen) and streptavidin conjugated with Alexa488 (Invitrogen).

Microscopy

Cells and GFP-encapsidated LENA were imaged by confocal fluorescence microscopy (LSM510 Meta 40× NA 1.4 lens; Carl Zeiss MicroImaging Inc., Tokyo, Japan).

Colorimetric detection of BlaM activity

Transfected 293T cells grown in 6 cm dishes were lysed in 500 μl of buffer A (10 mM HEPES, 1.5 mM $MgCl_2$, 10 mM KCl and 0.05% IGEPAL CA-630), and then 1 μl of nitrocefin (10 μg ml^{-1}; Calbiochem, San Diego, CA, USA) was added to the cell lysate. The mixture was incubated for 20 min at 37 °C.

Protein transduction

The pseudoinfection was performed as infecting cells with retroviral vectors[20] by incubating ~1×10^6 cells with 1 ml LENA-containing culture medium at 37 °C for 1–3 h in the presence of dextran (final concentration 16.25 μg ml^{-1}; DEAE-Dextran chloride, molecular weight ~500 kDa; ICN Biomedicals Inc., Aurora, OH, USA). The cells were assayed by flow cytometry or fluorescent microscopy after the LENA exposure. Bafilomycin A1 was purchased from Sigma.

Fluorescent detection of BlaM activity

A fluorescence-activated cell sorter Aria (Becton Dickinson, San Jose, CA, USA) was used to detect the CCF2-AM (Invitrogen) signals from 293T cells. A violet 407 nm laser was used for fluorescence activation, and BP450/40 nm and LP502 in conjunction with BP530/30 filters were used for the fluorescent signal detection of cleaved and uncleaved substrates, respectively. The CCF2-AM signals from 293T and MT-4 cells were imaged by Biorevo (BZ-9000, Keyence, Osaka, Japan) using the blue filter set (excitation, band pass filters 377/50 nm wavelength; emission, band pass 447/60 nm wavelength; dichroic mirror, 409 nm wavelength) and the green filter set (excitation, band pass filters 377/50 nm wavelength; emission, band pass 520/35 nm wavelength; dichroic mirror, 495 nm wavelength).

CONFLICT OF INTEREST

The authors declare no conflict of interest.

ACKNOWLEDGEMENTS

This work was supported by the Japan Health Science Foundation, the Japanese Ministry of Health, Labor, and Welfare (H18-AIDS-W-003 to JK) and the Japanese Ministry of Education, Culture, Sports, Science and Technology (18689014 and 18659136 to JK).

1 MacGregor RR. Clinical protocol. A phase 1 open-label clinical trial of the safety and tolerability of single escalating doses of autologous CD4 T cells transduced with VRX496 in HIV-positive subjects. *Hum Gene Ther* 2001; **12**: 2028–2029.
2 Cockrell AS, Kafri T. Gene delivery by lentivirus vectors. *Mol Biotechnol* 2007; **36**: 184–204.
3 McCart JA, Bartlett DI. Lentiviral Vectors. In: Templeton NS (ed.). *Gene and Cell Therapy: Therapeutic Mechanisms and Strategies*, 3rd edn. CRC Press: Carrollton, 2008, pp 245–262.
4 Lundberg C, Björklund T, Carlsson T, Jakobsson J, Hantraye P, Déglon N *et al.* Applications of lentiviral vectors for biology and gene therapy of neurological disorders. *Curr Gene Ther* 2008; **8**: 461–473.
5 Jacks T, Power MD, Masiarz FR, Luciw PA, Barr PJ, Varmus HE. Characterization of ribosomal frameshifting in HIV-1 gag-pol expression. *Nature* 1988; **331**: 280–283.
6 Klein KC, Reed JC, Lingappa JR. Intracellular destinies: degradation, targeting, assembly, and endocytosis of HIV Gag. *AIDS Rev* 2007; **9**: 150–161.
7 Briggs JA, Simon MN, Gross I, Kräusslich HG, Fuller SD, Vogt VM *et al.* The stoichiometry of Gag protein in HIV-1. *Nat Struct Mol Biol* 2004; **11**: 672–675.
8 Wyma DJ, Jiang J, Shi J, Zhou J, Lineberger JE, Miller MD *et al.* Coupling of human immunodeficiency virus type 1 fusion to virion maturation: a novel role of the gp41 cytoplasmic tail. *J Virol* 2004; **78**: 3429–3435.
9 Urano E, Aoki T, Futahashi Y, Murakami T, Morikawa Y, Yamamoto N *et al.* Substitution of the myristoylation signal of human immunodeficiency virus type 1 Pr55Gag with the phospholipase C-delta1 pleckstrin homology domain results in infectious pseudovirion production. *J Gen Virol* 2008; **89**: 3144–3149.
10 Aoki T, Shimizu S, Urano E, Futahashi Y, Hamatake M, Tamamura H *et al.* Improvement of lentiviral vector-mediated gene transduction by genetic engineering of the structural protein Pr55(Gag). *Gene Therapy* 2010; **17**: 1124–1133.
11 Voelkel C, Galla M, Maetzig T, Warlich E, Kuehle J, Zychlinski D *et al.* Protein transduction from retroviral Gag precursors. *Proc Natl Acad Sci USA* 2010; **107**: 7805–7810.
12 Hubner W, Chen P, Del Portillo A, Liu Y, Gordon RE, Chen BK. Sequence of human immunodeficiency virus type 1 (HIV-1) Gag localization and oligomerization monitored with live confocal imaging of a replication-competent, fluorescently tagged HIV-1. *J Virol* 2007; **81**: 12596–12607.
13 Campbell RE. Realization of beta-lactamase as a versatile fluorogenic reporter. *Trends Biotechnol* 2004; **22**: 208–211.
14 Wagner R, Graf M, Bieler K, Wolf H, Grunwald T, Foley P *et al.* Rev-independent expression of synthetic gag-pol genes of human immunodeficiency virus type 1 and simian immunodeficiency virus: implications for the safety of lentiviral vectors. *Hum Gene Ther* 2000; **11**: 2403–2413.
15 Ulett GA, Han S, Han JS. Electroacupuncture: mechanisms and clinical application. *Biol Psychiatry* 1998; **44**: 129–138.
16 Ford KG, Souberbielle BE, Darling D, Farzaneh F. Protein transduction: an alternative to genetic intervention? *Gene Therapy* 2001; **8**: 1–4.
17 Zhang Y, Yu LC. Microinjection as a tool of mechanical delivery. *Curr Opin Biotechnol* 2008; **19**: 506–510.
18 Cavrois M, De Noronha C, Greene WC. A sensitive and specific enzyme-based assay detecting HIV-1 virion fusion in primary T lymphocytes. *Nat Biotechnol* 2002; **20**: 1151–1154.
19 Yamanaka S, Blau HM. Nuclear reprogramming to a pluripotent state by three approaches. *Nature* 2010; **465**: 704–712.
20 Komano J, Miyauchi K, Matsuda Z, Yamamoto N. Inhibiting the Arp2/3 complex limits infection of both intracellular mature vaccinia virus and primate lentiviruses. *Mol Biol Cell* 2004; **15**: 5197–5207.
21 Stauffer TP, Ahn S, Meyer T. Receptor-induced transient reduction in plasma membrane PtdIns(4,5)P2 concentration monitored in living cells. *Curr Biol* 1998; **8**: 343–346.
22 Miyauchi K, Komano J, Yokomaku Y, Sugiura W, Yamamoto N, Matsuda Z. Role of the specific amino acid sequence of the membrane-spanning domain of human immunodeficiency virus type 1 in membrane fusion. *J Virol* 2005; **79**: 4720–4729.

Journal of Virological Methods 174 (2011) 131–135

Contents lists available at ScienceDirect

Journal of Virological Methods

journal homepage: www.elsevier.com/locate/jviromet

Short communication

Purification and concentration of non-infectious West Nile virus-like particles and infectious virions using a pseudo-affinity Cellufine Sulfate column

Naohiro Ohtaki[a], Hidehiro Takahashi[a], Keiko Kaneko[a], Yasuyuki Gomi[b], Toyokazu Ishikawa[b], Yasushi Higashi[b], Masami Todokoro[c], Takeshi Kurata[a], Tetsutaro Sata[a], Asato Kojima[a,*]

[a] Department of Pathology, National Institute of Infectious Diseases, Toyama 1-23-1, Shinjuku-ku, Tokyo 162-8640, Japan
[b] Kanonji Institute, The Research Foundation for Microbial Diseases of Osaka University, Yahata-cho, Kanonji-shi, Kagawa 768-0061, Japan
[c] Chemical Division, Chisso Corporation, Chiyoda-ku, Tokyo 100-8105, Japan

Article history:
Received 20 August 2010
Received in revised form 9 February 2011
Accepted 17 March 2011
Available online 1 April 2011

Keywords:
Cellufine Sulfate
West Nile virus
Particulate antigen
Column chromatography

A B S T R A C T

Affinity column chromatography is a promising method for the purification of flavivirus particles that can supplement or potentially replace diafiltration and sucrose density centrifugation. In this study, the purification of West Nile Virus (WNV) antigens via Cellufine Sulfate column chromatography was examined. Virus-like particles (VLPs) produced by the expression of the prM and E genes were separated from most of the contaminant proteins with 0.2–0.4 M NaCl, but still retained their spherical forms and immunogenicity in mice. The column, with a 1 mL bed-volume, concentrated WN-VLPs a minimum of 15 fold from culture supernatants. A heparin analogue, suramin, competitively eluted WN-VLPs, but sulphated polysaccharides, such as heparin, heparin sulfate and dextran sulfate, did not. Furthermore, 2.4×10^9 plaque forming units of WNV and 196 μg of the viral antigens were recovered from 60 mL of infected culture medium at high yields (93% and 96%, respectively). These results indicate that, in addition to conventional methods, Cellufine Sulfate column chromatography is an effective preparation technique for WNV particulate antigens that does not impair the antigen virological characteristics.

West Nile virus (WNV) is a member of the family *Flaviviridae* and genus *Flavivirus*, which includes some viruses important to public health: Japanese encephalitis virus (JEV), tick-borne encephalitis virus, dengue virus and yellow fever virus. WNV often causes febrile illness with a risk of severe meningoencephalitis in humans and has emerged as several outbreaks worldwide (Dauphin and Zientara, 2007). There is no antiviral drug or prophylactic vaccine effective against WNV for human use.

WNV virions are spherical, enveloped particles about 50 nm in diameter and composed of the capsid, envelope (E), membrane (M) proteins and the RNA genome. The expression of the E and precursor of M (prM) proteins produces small (20–30 nm), noninfectious virus-like particles (VLPs) or recombinant subviral particles (Hanna et al., 2005; Takahashi et al., 2009). The particle morphology of flaviviruses is thought to be important for effective antibody induction and protection against viral challenge (Heinz et al., 1995). Many WNV vaccine candidates have been developed in particulate forms: inactivated whole virions (Lim et al., 2008), propagation-defective viruses (Widman et al., 2008) and chimeric flaviviruses replaced with the WNV prM-E gene region (Monath et al., 2006; Pletnev et al., 2006). In addition, WN-VLP antigens have been developed as a novel subunit vaccine candidate (Takahashi et al., 2009; Ohtaki et al., 2010).

Particle-based flavivirus vaccines are manufactured commonly by purification techniques such as diafiltration and sucrose density gradient centrifugation (Ehrlich et al., 2003; Monath et al., 2006; Toriniwa and Komiya, 2008). However, these purification methods depend on physical properties like molecular size, density and buoyancy and are occasionally unreliable. It has been proposed that unidentified host proteins in the mouse brain-derived JEV vaccine that could not be removed by conventional methods caused acute disseminated encephalomyelitis in some recipients (Ohtaki et al., 1995). Therefore, additional purification steps are needed to improve the safety of vaccines. Column chromatography that depends on biochemical characteristics would be advantageous for purifying vaccine antigens.

In this study, a pseudo-affinity Cellufine Sulfate column (Chisso, Tokyo, Japan) was tested for purification of WNV particle antigens. The Cellufine Sulfate column and its related products have been shown to be effective for the purification of several DNA and RNA

* Corresponding author. Tel.: +81 3 5285 1111; fax: +81 3 5285 1189.
E-mail addresses: ohtaki@nih.go.jp (N. Ohtaki), htakahas@nih.go.jp (H. Takahashi), keiko5@nih.go.jp (K. Kaneko), ygomi@mail.biken.or.jp (Y. Gomi), toishika@mail.biken.or.jp (T. Ishikawa), yhigashi@mail.biken.or.jp (Y. Higashi), m.todokoro@chisso.co.jp (M. Todokoro), tkurata@nih.go.jp (T. Kurata), tsata@nih.go.jp (T. Sata), akojima@nih.go.jp (A. Kojima).

0166-0934/$ – see front matter © 2011 Elsevier B.V. All rights reserved.
doi:10.1016/j.jviromet.2011.03.021

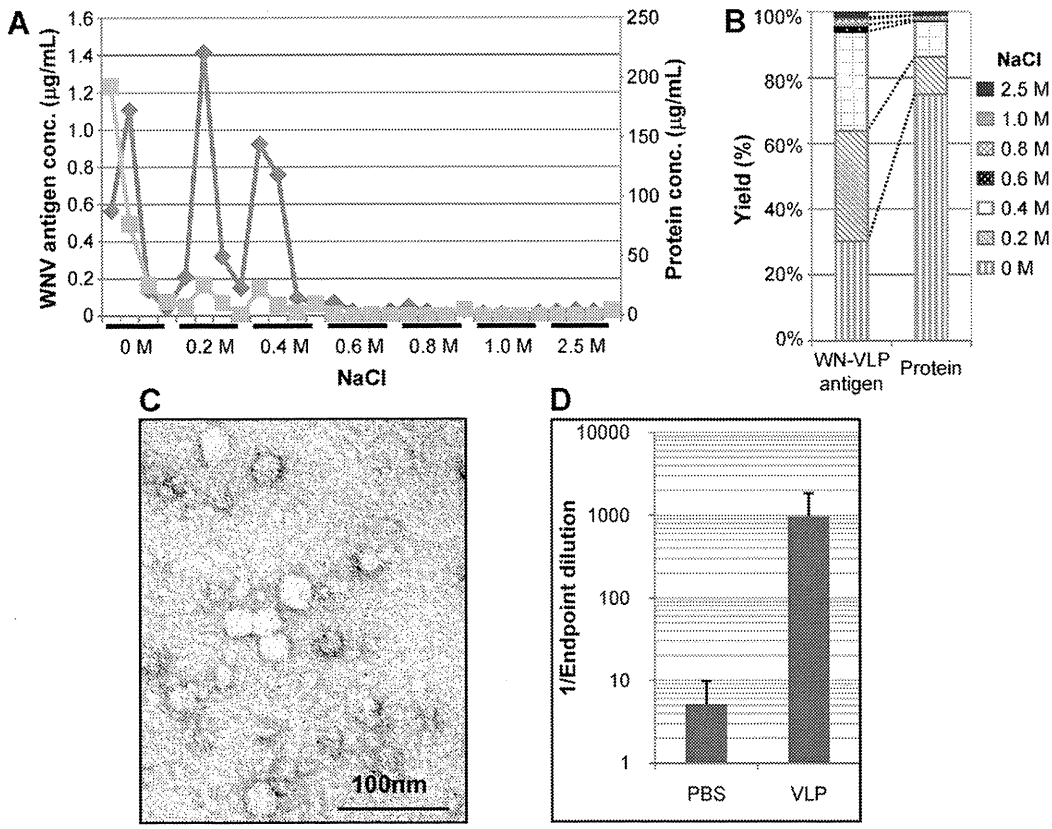

Fig. 1. Recovery of WN-VLPs by Cellufine Sulfate column chromatography. WN-VLPs released from #22.6 cells expressing constitutively the WNV prM-E gene were absorbed on a Cellufine Sulfate mini-column. The WNV antigens were eluted with the increasing NaCl concentration in 50 mM carbonate buffer (pH 9.2) and analysed by WNV-specific ELISA. The protein contents were determined by a Lowry protein assay. The peak fractions in 0.2 and 0.4 M NaCl were pooled, exchanged for PBS, concentrated and examined by electron microscopy and mouse immunization. (A) The elution patterns of WN-VLPs and proteins are represented by diamonds and squares, respectively. (B) Recoveries of WN-VLPs and proteins in (A) are summarized in build-up graphs where the total amounts of the eluted WNV antigens and proteins are defined as 100%. (C) An electron micrograph of the eluted WN-VLP antigens. (D) C3H/He mice were immunized twice with the eluted WN-VLP antigens in PBS. Sera were collected 7days after the second immunization. Titres of anti-WNV antibodies in mice were measured by IgG ELISA.

viruses, such as herpes simplex virus and measles virus (O'Neil and Balkovic, 1993), influenza virus (Opitz et al., 2009) and the human immunodeficiency virus (Bartz et al., 1994). Cellufine Sulfate is produced by the chemical modification of cellulose beads with a low concentration of sulfate ester and mimics sulphated polysaccharides, which are antiviral agents and are thought to interrupt viral entry into host cells by binding to the viral envelope proteins (Baba et al., 1988; Witvrouw and De Clercq, 1997). Indeed, heparin, heparan sulfate and dextran sulfate are reported to inhibit flavivirus infectivity proportional to their viral E protein-binding activity (Chen et al., 1997; Lee et al., 2006; Su et al., 2001). Thus, a sulphated cellulose column should be useful for the preparation of WNV antigen particles.

In an initial experiment, an attempt was made to determine whether WN-VLPs remain bound to Cellufine Sulfate in a carbonate buffer system, which is used for preparing formalin-inactivated JEV (Sugawara et al., 2002). WNV antigens were prepared from a CHO cell clone, #22.6, which expresses the WNV prM-E gene constitutively (Ohtaki et al., 2010). The #22.6 culture supernatant was concentrated by ultrafiltration, exchanged for 50 mM Tris–HCl (pH 7.5)-150 mM NaCl and applied to a Cellufine Sulfate mini-column (1 mL bed-volume). The bound WNV antigens were eluted in increasing concentrations (0, 0.2, 0.4, 0.6, 0.8, 1.0 and 2.5 M) of NaCl in 50 mM carbonate buffer (pH 9.2). Fig. 1A shows the elution patterns of the WNV antigens and proteins measured in each fraction (0.75 mL) by an antigen-capture enzyme-linked immunosorbent assay (ELISA), as described previously (Takahashi et al., 2009), and by a Lowry assay with a bovine serum albumin standard, respectively. The recoveries were calculated and summarized in Fig. 1B. Almost a third (~30%) of the WNV antigens was lost in a wash step with NaCl-free (0 M NaCl) carbonate buffer, though almost 75% of the total proteins were eluted from the column in the wash fractions. However, with 0.2–0.4 M NaCl, mostly viral antigens were eluted, and more than 60% of the antigens were recovered in these fractions with only small amounts of contaminant proteins. These results suggest that if an adequate buffer is selected, Cellufine Sulfate is suitable for binding WN-VLPs and separating them from the contaminant proteins with a moderate NaCl concentration.

The WNV antigens recovered from the Cellufine Sulfate column were transferred from a carbonate buffer to phosphate-buffered saline (PBS) with a PD-10 column (GE Healthcare UK Ltd, Buckinghamshire, England), concentrated by ultrafiltration and observed by electron microscopy. As shown in Fig. 1C, the eluted antigens appeared to be spherical particles 20–30 nm in diameter, which corresponds to the intact forms of WN-VLPs. To examine the immunogenicity of the VLP antigens, groups of four C3H/He mice were immunized twice with the WN-VLP preparation in PBS, and titres of anti-WNV immunoglobulin G (IgG) were measured by antibody ELISA, as described previously (Takahashi et al., 2009). Fig. 1D shows that the WN-VLP antigens induced anti-WNV IgG in mice, indicating that the VLP antigens retained their immunogenicity after preparation by affinity chromatography. From these results, Cellufine Sulfate was expected to be a useful tool for purifying WN-VLPs, and additional experiments were performed to establish the optimal pH and buffer conditions for use of the affinity column.

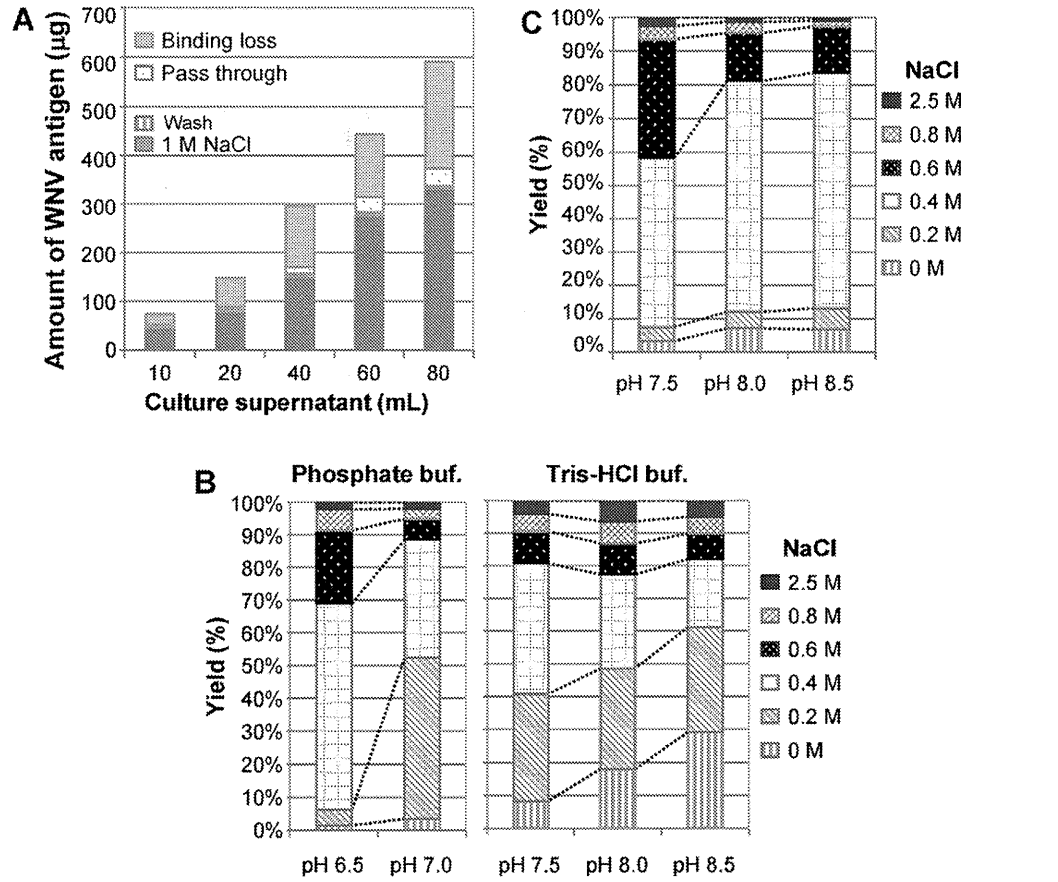

Fig. 2. The optimum conditions for preparing the WN-VLP antigens. Culture supernatants were collected from (A and B) serum-free medium of #22.6S cells or (C) FBS (10%)-containing medium of the parental #22.6 cells and applied to a mini-column. The amounts of WN-VLPs were determined by ELISA in the initial culture fluids and the effluents. (A) The mini-column was injected with increasing volume of the serum-free medium and washed with 50 mM Tris–HCl (pH 7.5). The bound antigens were eluted with 1 M NaCl in Tris–HCl. The "binding loss" represents the amount of WN-VLPs calculated by the total input minus the recovery in each fraction. (B) The effects of pH and NaCl concentration on the elution efficiency. A fixed volume (20 mL) of the serum-free culture medium of #22.6S cells was loaded to the column and eluted with various combinations of pH and NaCl concentration indicated. (C) Recovery of WN-VLPs from the FBS-containing culture medium of #22.6 cells was analysed at pH 7.5–8.5 as in (B).

The usefulness of the column for concentrating WN-VLPs was examined by direct injection of increasing volumes (10–80 mL) of the culture supernatant containing the VLP antigens (5–10 μg/mL), which was prepared from suspension cultures of the #22.6S cell clone adapted in serum-free SFM-II medium (Invitrogen, Grand Island, NY, USA) (Ohtaki et al., 2010). The binding capacity of the column (3 mg per 1 mL bed-volume) corresponds to the amount of WN-VLPs in 300–600 mL of the culture supernatant. The bound VLPs were washed with 4.5 mL of 50 mM Tris–HCl (pH 7.5) and eluted with 3 mL of buffer containing 1 M NaCl. The amounts of eluted WNV antigens increased proportionally with the increasing volumes of the culture medium. About 330 μg of the antigen was recovered from 80 mL of the culture supernatant and concentrated about 15 fold, from 7.4 to 110 μg/mL (Fig. 2A). These results indicate that Cellufine Sulfate can be effective for concentrating WN-VLPs from culture supernatants.

The influence of the elution buffer pH on WN-VLP recovery was examined by altering the ionic strength of the buffer to diminish the interactions between the VLP antigens and Cellufine Sulfate. Equal volumes (20 mL) of the #22.6S serum-free culture supernatant were applied to the mini-columns and eluted with 50 mM phosphate buffer (pH 6.5 or 7.0) or 50 mM Tris–HCl buffer (pH 7.5, 8.0 or 8.5) containing 0–2.5 M NaCl. Considerable amounts of WN-VLPs were eluted using phosphate buffer and (pH 7.0) 0.2 M NaCl. In addition, the highest amounts of WN-VLPs were recovered in phosphate buffer at pH 7.0 containing 0.4 M NaCl. However, without NaCl, increasing the pH from 7.5 to 8.5 in Tris–HCl buffer eluted increasing amounts of the VLP antigens in wash fractions (Fig. 2B). Alternative pH and NaCl concentrations were required to elute WN-VLPs that derived from parental #22.6 cell cultures in serum-containing medium (Fig. 2C). WN-VLP recovery was inefficient in Tris–HCl (pH 7.5–8.5) with 0.2 M NaCl. A higher NaCl concentration of 0.6 M was needed to achieve an 80–90% recovery of WN-VLPs at pH 7.5–8.5 (Fig. 2C). Taken together, phosphate buffer (pH 7.0) with 0.4 M NaCl seems to be adequate for recovery, and higher pH facilitates dissociation of WN-VLPs from Cellufine Sulfate. However, the producer cells and/or culture medium of the VLP antigens may still modulate the binding affinity.

The binding characteristics between WN-VLPs and Cellufine Sulfate were examined by competitive elution with sulphated polysaccharides (heparin, heparan sulfate and dextran sulfate) and a heparin analogue (suramin) (Sigma–Aldrich, St. Louis, MO, USA). Suramin is a symmetric molecule with the framework composed of 4 benzene and 2 naphthalene rings instead of polysaccharides (Fig. 3A). WN-VLPs bound to the column were eluted with increasing concentrations of the competitors from 1 to 100 μg/mL in PBS. All the competitors examined have been reported to inhibit flavivirus infection in the range of 1–100 μg/mL (Chen et al., 1997; Lee et al., 2006; Su et al., 2001). However, none of the sulphated glycans desorbed WN-VLPs by more than 20%. In contrast, suramin effectively eluted WN-VLPs, and more than 80% of the antigens were recovered with 100 μg/mL of this sulphated compound (Fig. 3B). These results suggest that the interaction of WN-VLPs with Cellufine Sulfate differs

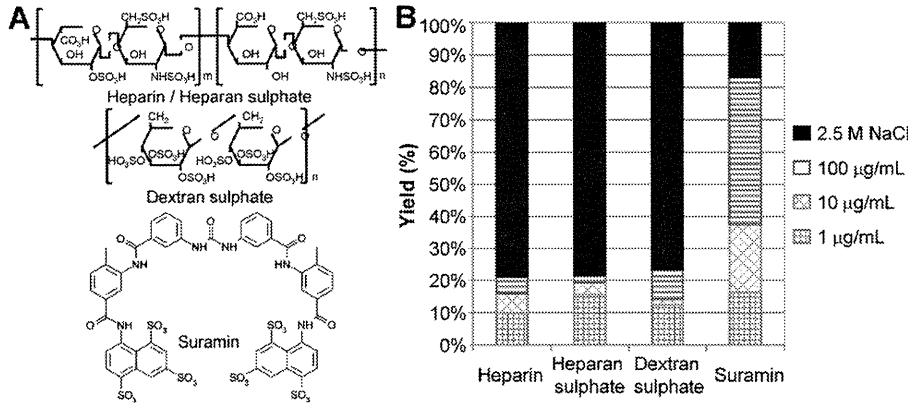

Fig. 3. Competitive elution of WN-VLPs from Cellufine Sulfate. (A) The chemical structures of heparin/heparin sulfate, dextran sulfate and suramin. (B) WN-VLPs from #22.6S cell cultures were adsorbed, washed with PBS and eluted with increasing concentrations of the sulphated competitors. All the remaining VLP antigens were desorbed with 2.5 M NaCl from a Cellufine Sulfate column. The results are expressed as % of the total amount of the bound WN-VLP antigens.

from that of the sulphated polysaccharides but mimics that of suramin.

Finally, the recovery of infectious WNV particles was examined. WNV was propagated on Vero E6 cell monolayers in serum-free VP-SFM (Invitrogen, Grand Island, NY, USA) medium. Viral infectivity and WNV antigen amounts in Tris–HCl (pH 7.5)–1 M NaCl effluents were measured by a plaque assay and ELISA, respectively. As depicted in Fig. 4A, the recoveries of both infectious virus and the viral antigens increased with the increasing volume of the infected culture fluids. About 2.4×10^9 plaque forming units (pfu) of WNV, corresponding to about 200 μg of the antigen, was obtained from 60 mL of the culture supernatant that contained initially 2.6×10^9 pfu of infectious WNV and 204 μg of the viral antigen. Thus, the yield of infectious virus particles was 70%, 63% and 93% for 15, 30 and 60 mL of the infected culture supernatant, respectively. The effects of pH and NaCl concentration on the yield of infectious WNV were analysed as described for non-infectious WN-VLPs in Fig. 2B. Only 20–30% of infectivity, corresponding to 10% of the viral antigens, was obtained with 50 mM Tris–HCl (pH 7.5)–0.2 M NaCl. At pH 9.0 in 50 mM carbonate buffer, however, 90% of the input infectivity and viral antigens was recovered in 0.75 mL of 0.2 M NaCl fraction (Fig. 4B). From these results, Cellufine Sulfate appears to be useful for concentrating and purifying infectious WNV virions from cultures without causing viral inactivation.

Initial viral materials from cell cultures usually contain virions or VLPs at a low concentration with large amounts of contaminant impurities. The first step for purifying the viral antigens is to concentrate them by reducing sample volume. Polyethylene glycol precipitation also collects host cell-derived contaminants. Diafiltration is easy to implement, but pores of the filters are sometimes clogged with aggregates from cell cultures. Sucrose density centrifugation, the most convenient method for virus preparation, is inadequate for purifying WN-VLPs because a sucrose concentration of over 30% disrupts WN-VLP particle structures and impairs their immunogenicity, as described previously (Ohtaki et al., 2010). For processing large volumes of culture fluids, continuous-flow ultracentrifugation has been used, but requires expensive centrifuge equipment and a large investment of time. In addition, ultracentrifugation can potentially generate considerable safety hazards when preparing infectious particles. Immunoaffinity chromatography using immobilized antibodies has the potential to be the most efficient method, but acidic elution buffers, often at pH 2.6, would likely impair infectivity of WNV and immunogenicity of WN-VLPs because flaviviruses are known to be highly sensitive to acidic pH (Schalich et al., 1996). Cellufine Sulfate chromatography can overcome these problems.

This study has demonstrated that Cellufine Sulfate can bind, concentrate and separate WNV particulate antigens from contaminant proteins under moderate salt and pH conditions. As 30% of WNV antigens were lost during wash steps with carbonate buffer (pH 9.2), used for preparing formalin-inactivated JEV (Sugawara et al., 2002), such a buffer seems to be unsuitable for efficient recovery of WN-VLPs. However, the recovered antigens retained their intact spherical forms and immunogenicity after the buffer change to PBS (Fig. 1). In addition, phosphate buffer (pH 7.0), a buffer advantageous for immunization, appears to be optimal for eluting

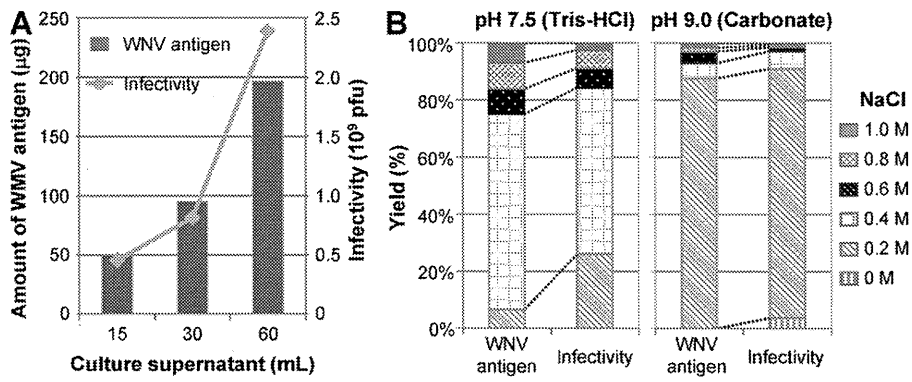

Fig. 4. The concentration and purification of infectious WNV virions. WNV was propagated on Vero cell monolayers in serum-free medium, bound to a Cellufine Sulfate column and eluted with 0–1 M NaCl. Viral infectivity and amounts of the WNV antigens were measured by a plaque assay and ELISA, respectively. (A) The viral infectivity and amount of WNV antigen in the 1 M NaCl effluents are presented by diamonds and bars, respectively. (B) The build-up graphs summarize the effects of pH and NaCl concentration on the yields of virus infectivity and WNV antigens.

WN-VLPs (Fig. 2). Thus, Cellufine Sulfate column chromatography is applicable to the production of non-infectious WN-VLPs and formalin-inactivated whole virions for particle-based WNV vaccines. Notably, infectious WNV was also recovered without loss of viral infectivity (Fig. 4), suggesting that a Cellufine Sulfate column could aid in the effective preparation of live vaccines, such as the promising chimeric virus and single-cycle virus vaccine candidates.

Sulfate ester residues on Cellufine Sulfate beads contribute to ionic interaction with the positively charged E protein on the surface of WNV antigen particles. A highly sulphated compound, suramin, competitively eluted WN-VLPs from the sulphated matrix, but other highly sulphated glycans, such as heparin, heparan sulfate and dextran sulfate, did not (Fig. 3). Although the reasons for the inefficient elution by the sulphated polysaccharides are unknown, it is possible that the difference in the backbone structures, a symmetric framework with 4 benzene/2 naphthalene rings or disaccharide polymer chains, might affect the desorption of WN-VLPs from negatively charged Cellufine Sulfate.

The ionic interaction between the WNV antigens and Cellufine Sulfate seems to depend on pH rather than NaCl concentration. WN-VLPs were eluted during wash steps at an increasing pH from 7.5 to 8.5 without NaCl and were more effectively eluted at a basic pH with 0.2–0.4 M NaCl (Fig. 2). Higher NaCl concentration, however, affected the yields slightly. Conversely, the yield at pH 6.5 was dramatically low compared to the yield at pH 7.0, suggesting that acidic pH conditions strengthen the binding affinity of the WNV antigens. The conformation of the E protein arranged on the surface of WNV particles is likely changed at a pH below 6.5, a phenomenon observed in other flavivirus E proteins (Schalich et al., 1996).

In conclusion, Cellufine Sulfate column chromatography is suitable for the effective purification and concentration of VLPs and live vaccine antigens of WNV. The technique preserves the virological properties of the antigens, the intact particulate forms, immunogenicity and infectivity. Cellufine sulfate chromatography can be easily used in addition to other conventional virus purification methods. Furthermore, this study will provide helpful information on how to prepare optimum conditions for the production of high-yield VLPs and the infective virions of non-WNV flaviviruses.

Acknowledgements

This work was supported in part by research grants from the Ministry of Health, Labour and Welfare and from the Japanese Health Sciences Foundation.

References

Baba, M., Snoeck, R., Pauwels, R., de Clercq, E., 1988. Sulfated polysaccharides are potent and selective inhibitors of various enveloped viruses, including herpes simplex virus, cytomegalovirus, vesicular stomatitis virus, and human immunodeficiency virus. Antimicrob. Agents Chemother. 32, 1742–1745.

Bartz, S.R., Pauza, C.D., Ivanyi, J., Jindal, S., Welch, W.J., Malkovsky, M., 1994. An Hsp60 related protein is associated with purified HIV and SIV. J. Med. Primatol. 23, 151–154.

Chen, Y., Maguire, T., Hileman, R.E., Fromm, J.R., Esko, J.D., Linhardt, R.J., Marks, R.M., 1997. Dengue virus infectivity depends on envelope protein binding to target cell heparan sulfate. Nat. Med. 3, 866–871.

Dauphin, G., Zientara, S., 2007. West Nile virus: recent trends in diagnosis and vaccine development. Vaccine 25, 5563–5576.

Ehrlich, H.J., Pavlova, B.G., Fritsch, S., Poellabauer, E.M., Loew-Baselli, A., Obermann-Slupetzky, O., Maritsch, F., Cil, I., Dorner, F., Barrett, P.N., 2003. Randomized, phase II dose-finding studies of a modified tick-borne encephalitis vaccine: evaluation of safety and immunogenicity. Vaccine 22, 217–223.

Hanna, S.L., Pierson, T.C., Sanchez, M.D., Ahmed, A.A., Murtadha, M.M., Doms, R.W., 2005. N-linked glycosylation of West Nile virus envelope proteins influences particle assembly and infectivity. J. Virol. 79, 13262–13274.

Heinz, F.X., Allison, S.L., Stiasny, K., Schalich, J., Holzmann, H., Mandl, C.W., Kunz, C., 1995. Recombinant and virion-derived soluble and particulate immunogens for vaccination against tick-borne encephalitis. Vaccine 13, 1636–1642.

Lee, E., Pavy, M., Young, N., Freeman, C., Lobigs, M., 2006. Antiviral effect of the heparan sulfate mimetic PI-88, against dengue and encephalitic flaviviruses. Antiviral Res. 69, 31–38.

Lim, C.K., Takasaki, T., Kotaki, A., Kurane, I., 2008. Vero cell-derived inactivated West Nile (WN) vaccine induces protective immunity against lethal WN virus infection in mice and shows a facilitated neutralizing antibody response in mice previously immunized with Japanese encephalitis vaccine. Virology 374, 60–70.

Monath, T.P., Liu, J., Kanesa-Thasan, N., Myers, G.A., Nichols, R., Deary, A., McCarthy, K., Johnson, C., Ermak, T., Shin, S., Arroyo, J., Guirakhoo, F., Kennedy, J.S., Ennis, F.A., Green, S., Bedford, P., 2006. A live, attenuated recombinant West Nile virus vaccine. Proc. Natl. Acad. Sci. U.S.A. 103, 6694–6699.

Ohtaki, E., Matsuishi, T., Hirano, Y., Maekawa, K., 1995. Acute disseminated encephalomyelitis after treatment with Japanese B encephalitis vaccine (Nakayama-Yoken and Beijing strains). J. Neurol. Neurosurg. Psychiatry 59, 316–317.

Ohtaki, N., Takahashi, H., Kaneko, K., Gomi, Y., Ishikawa, T., Higashi, Y., Kurata, T., Tetsutaro Sata, T., Kojima, A., 2010. Immunogenicity and efficacy of two types of West Nile virus-like particles different in size and maturation as a second-generation vaccine candidate. Vaccine 28, 6588–6596.

O'Neil, P.F., Balkovic, E.S., 1993. Virus harvesting and affinity-based liquid chromatography A method for virus concentration and purification. Biotechnology (N. Y.) 11, 173–178.

Opitz, L., Lehmann, S., Reichl, U., Wolff, M.W., 2009. Sulfated membrane adsorbers for economic pseudo-affinity capture of influenza virus particles. Biotechnol. Bioeng. 103, 1144–1154.

Pletnev, A.G., Swayne, D.E., Speicher, J., Rumyantsev, A.A., Murphy, B.R., 2006. Chimeric West Nile/dengue virus vaccine candidate: preclinical evaluation in mice, geese and monkeys for safety and immunogenicity. Vaccine 24, 6392–6404.

Schalich, J., Allison, S.L., Stiasny, K., Mandl, C.W., Kunz, C., Heinz, F.X., 1996. Recombinant subviral particles from tick-borne encephalitis virus are fusogenic and provide a model system for studying flavivirus envelope glycoprotein functions. J. Virol. 70, 4549–4557.

Su, C.M., Liao, C.L., Lee, Y.L., Lin, Y.L., 2001. Highly sulfated forms of heparin sulfate are involved in Japanese encephalitis virus infection. Virology 286, 206–215.

Sugawara, K., Nishiyama, K., Ishikawa, Y., Abe, M., Sonoda, K., Komatsu, K., Horikawa, Y., Takeda, K., Honda, T., Kuzuhara, S., Kino, Y., Mizokami, H., Mizuno, K., Oka, T., Honda, K., 2002. Development of Vero cell-derived inactivated Japanese encephalitis vaccine. Biologicals 30, 303–314.

Takahashi, H., Ohtaki, N., Maeda-Sato, M., Tanaka, M., Tanaka, K., Sawa, H., Ishikawa, T., Takamizawa, A., Takasaki, T., Hasegawa, H., Sata, T., Hall, W.W., Kurata, T., Kojima, A., 2009. Effects of the number of amino acid residues in the signal segment upstream or downstream of the NS2B-3 cleavage site on production and secretion of prM/M-E virus-like particles of West Nile virus. Microbes Infect. 11, 1019–1028.

Toriniwa, H., Komiya, T., 2008. Long-term stability of Vero cell-derived inactivated Japanese encephalitis vaccine prepared using serum-free medium. Vaccine 26, 3680–3689.

Widman, D.G., Ishikawa, T., Fayzulin, R., Bourne, N., Mason, P.W., 2008. Construction and characterization of a second-generation pseudoinfectious West Nile virus vaccine propagated using a new cultivation system. Vaccine 26, 2762–2771.

Witvrouw, M., De Clercq, E., 1997. Sulfated polysaccharides extracted from sea algae as potential antiviral drugs. Gen. Pharmacol. 29, 497–511.

Induction of extremely low protein expression level by fusion of *C*-terminal region of Nef

Nobutoki Takamune[*1], Yukari Irisaka[*], Minami Yamamoto[*], Keisuke Harada[*], Shozo Shoji[*U], and Shogo Misumi[*]

[*]Department of Pharmaceutical Biochemistry, Faculty of Life Sciences, Kumamoto University, 5-1 Oe-Honmachi, Kumamoto 862-0973, Japan. [U]Kumamoto Health Science University, Kumamoto, 325 Izumimachi, Kumamoto 861-5598, Japan.

Running title : Induction of extremely low protein expression level

Address correspondence to: Nobutoki Takamune, PhD, 5-1 Oe-Honmachi, Kumamoto 862-0973, Japan.
Phone: +81-96-371-4367
Fax: +81-96-362-7800
E-mail: tkmnnbtk@gpo.kumamoto-u.ac.jp

Synopsis

Nef is one of the accessory proteins of human immunodeficiency viruses. Here, we noted that the relative expression level of Nef_{NL4-3} is much lower than that of Nef_{JR-CSF} in HEK293 cells. By evaluating the expression level using a Nef mutant, it was indicated that amino acids 129-206 of Nef_{NL4-3}, i.e., the *C*-terminal region named NLAA129-206, could contain the region responsible for the induction of the low protein expression level. Additionally, the expression levels of the enhanced green fluorescent protein (EGFP) and *Renilla* luciferase (Rluc) became extremely low with the fusion of NLAA129-206, Interestingly, the NLAA129-206-corresponding sequences of other Nef variants with relatively high expression levels also induced the extremely low protein expression level by fusion. These results suggest that the *C*-terminal region of Nef can generally induce an extremely low protein expression level. Here, we propose that the *C*-terminal region of Nef could become an excellent tool for the induction of an extremely low expression level of arbitrary proteins by attachment as fusion proteins.

Footnotes

Key words: enhanced green fluorescent protein (EGFP), human immunodeficiency virus (HIV), Nef, protein degradation sequence, *Renilla* luciferase (Rluc).

Abbreviations used: HIV, human immunodeficiency virus; SIV, simian immunodeficiency virus; HEK293, human embryonic kidney 293; EGFP, enhanced green fluorescent protein; Rluc, *Renilla* luciferase; DAPI, 4',6-diamidino-2-phenylindole dihydrochloride; SDS-PAGE, sodium dodecyl sulfate-polyacrylamide gel electrophoresis; UPS, ubiquitin proteasome system

[1]To whom correspondence should be address (email: tkmnnbtk@gpo.kumamoto-u.ac.jp)

Introduction

Nef, a 27-35-kDa protein, is one of the accessory proteins of human and simian immunodeficiency viruses (HIV and SIV, respectively) that enhance viral replication and is associated with the pathogenicity of these viruses. It has many functional motifs for contact to host proteins [1], by which it can serve as a molecular adaptor and exert multiple functions like CD4 downregulation and MHC class I downregulation [2]. Moreover, Nef can enhance viral infectivity, although the mechanism underlying such enhancement remains unclear [3]. *N*-myristoylation occurs at the *N*-terminus of Nef [4], and the posttranslational modification is essential for multiple functions [2].

Genetic diversity is one of the major characteristics of HIV and SIV [5]. We can find highly frequent mutations of amino acid substitution, insertion, and deletion among viral strains in the Los Alamos HIV database (http://hiv-web.lanl.gov). Such a genetic diversity can generate many viral phenotypes, resulting in, for example, CCR5 or CXCR4 usage [6], escape from the immune attack of the host [7], and the emergence of drug-resistant viruses [7].

The abundance of each protein is closely associated with the efficacy of its function, because protein activity is basically exerted in a dose-dependent manner. Protein expression level depends not only on mRNA level but also on translation rate and degradation rate [8, 9]. Protein degradation comprises two major systems: ubiquitin-mediated proteolysis and lysosomal degradation [10].

Some degradation signals conferring instability on proteins have been found, which include N-degrons [11], a murine ornithine decarboxylase (MODC) PEST region [12], and CL peptides [13]. These signals induce a rapid protein degradation mediated by a proteasome, in which the N-degron and CL peptides require ubiquitination

prior to degradation, while the PEST sequence is independent of ubiqutination [14]. The PEST sequence and CL peptides could convert stable proteins into unstable proteins by attachment as fusion proteins [13, 15,16], of which the apparent expression levels could be much lower than those of the original proteins [15-17]. The feature of the instability induction of the PEST sequence and CL peptides has been applied to the development of a highly responsive reporter system [18-20] and to the improvement of the recombinant protein productivity of CHO cells [21]. In addition to protein degradation signals, mRNA-destabilizing elements [22-24] are utilized for such a system [18].

Here, we clarified that the *C*-terminal region (amino acids 129-206) of Nef_{NL4-3} with an extremely low expression level is necessary and sufficient for the induction of the low expression level of reporter proteins by attachment as fusion proteins. Additionally, it was indicated that the *C*-terminal regions of not only Nef_{NL4-3} but also other Nef variants, which even show relatively higher expression levels, have an ability to induce low protein expression levels by attachment. The mechanism of this induction has not been fully resolved yet. We propose that the *C*-terminal region of Nef is applicable to the development of a highly responsive reporter system and to the improvement of recombinant protein productivity.

Materials and Methods

Nef expression vectors

DNAs coding Nef proteins were amplified by PCR using the corresponding proviral DNA template and subcloned into pcDNA^{TM}3.1D/V5-His TOPO according to the manufacturer's instructions (Invitrogen, Carlsbad, CA).

DNA coding Nef_{JR-CSF}-V5 or Nef_{NL4-3}-V5 was amplified by PCR using pcDNA3.1/Nef_{JR-CSF}-V5 and pcDNA3.1/Nef_{NL4-3}-V5, respectively, and subcloned into the pcDNA4/HisMax vector (Invitrogen, Carlsbad, CA) without polyhistidine and the Xpress^{TM} epitope-coding region. The expression vector for the Nefchimera was generated by standard overlapping PCR techniques [25].

The expression vector for each Nef Gly 2-to-Ala 2 (G2A) mutant was constructed by site-directed mutagenesis, as previously described [26].

Expression vectors of enhanced green fluorescent protein (EGFP) or *Renilla* luciferase (Rluc) fusion protein

Each expression vector for EGFP appended with each amino acid sequence to the *N*-terminal end was constructed using pEGFP-N1 (Clontech, Mountain View, CA), in which a triple repeat of the linker Gly-Gly-Gly-Gly-Ser [$(GGGGS)_3$] [27] and Xpress-epitope-tag-coding DNAs were respectively inserted at the *Sal*I-*Apa*I and *Hin*dIII-*Pst*I sites. Each expression vector for Rluc was constructed by replacing the EGFP-coding DNA with the Rluc-coding DNA of the multiple cloning site (MCS) of each EGFP expression vector. Each expression vector for EGFP appended with each amino acid sequence to the *C*-terminal end was constructed using a pcDNA4/HisMax vector, in which EGFP, the $(GGGGS)_3$ linker, and DNAs coding each amino acid sequence were respectively inserted in the *Kpn*I-*Bam*HI, *Bam*HI-*Eco*RI, and *Eco*RI-*Pst* I sites of the MCS of the vector.

Cell culture and transfection

Human embryonic kidney 293 (HEK293) cells were cultured and transfected using Lipofectamine LTX reagent, as previously described [26].

HEK293/CD4/Nef_{JR-CSF}, HEK293/CD4/Nef_{NL4-3}, HEK293/CD4/Nef_{JR-CSF} G2A, and HEK293/CD4/Nef_{NL4-3} G2A cells

HEK293/CD4 cells were transfected with the pcDNA4/HisMax vector for Nef_{JR-CSF}, Nef_{NL4-3}, Nef_{JR-CSF} G2A, and Nef_{NL4-3} G2A. 2 days after transfection, stable clones were selected in the presence of 500 μg/ml zeocin in the conditioned medium. Each clonal HEK293/CD4/Nef cell line was obtained by the limiting-dilution method.

Immunostaining analysis

The cells were rinsed and fixed with 1% fresh paraformaldehyde in PBS(-). After permeabilization with methanol, Nef was visualized using an anti-V5 antibody, followed by an anti-mouse-FITC secondary antibody. The nucleus was stained with 4',6-diamidino-2-phenylindole dihydrochloride (DAPI). The cells were observed using a Biozero digital microscope (Keyence, Osaka, Japan).

Cell lysis and western blot analysis

The cells were lysed in lysis buffer (50 mM Tris-HCl pH 8.0, 150 mM NaCl, 1% Triton X-100, protease inhibitors [1 mM 4-amidinophenylmethanesulfonyl fluoride hydrochloride (APMSF), 50 μg/ml aprotinin, 50 μg/ml leupeptin, 50 μg/ml pepstatin A, 50 μg/ml antipine]) and subjected to 5-20% polyacrylamide gradient sodium dodecyl sulfate-polyacrylamide gel electrophoresis (SDS-PAGE). Then, separated proteins on the gel were transferred to the polyvinylidene fluoride (PVDF) membrane. The membranes blocked by 5% skim-milk were incubated with an anti-V5 antibody or anti-Xpress antibody (Invitrogen, Carlsbad, CA) diluted 1:5000 in immunoenhancer reagent A (Wako, Osaka, Japan) for 4 h, and then with peroxidase (POD) conjugated

anti-mouse IgG in immunoenhancer reagent B (Wako) for 1 h. Then, the specific signals were observed using chemiluminescent substrate (Thermo Fisher Scientific inc., Waltham, MA) and LAS4000 (GE Healthcare), as previously described [28]. The intensities of the bands were quantified with Fujifilm Image Gauge Software.

Rluc assay

HEK293 cells were transiently transfected with each Rluc-fusion-protein expression vector and cultured for 48 h. The harvested cells (1 x 10^5 cells) were lysed with the cell culture lysis reagent (Promega, Madison, WI). To measure Rluc activity, each lysate was transferred to a 96-well white microplate and coelenterazine h [29] was added at a final concentration of 5 μM. Then, luminescence was measured simultaneously using a Wallac ARVO™ SX 1420 luminometer (Perkin-Elmer, Waltman, MA).

Flow cytometry

HEK293/CD4/$Nef_{JR\text{-}CSF}$, HEK293/CD4/$Nef_{NL4\text{-}3}$, HEK293/CD4/$Nef_{JR\text{-}CSF}$ G2A, and HEK293/CD4/$Nef_{NL4\text{-}3}$ G2A cells were washed with PBS and then suspended in a cold washing buffer (PBS containing 2% FCS and 0.02% NaN_3) containing a phycoerythrin (PE)-conjugated anti-CD4 antibody. After 30 min of incubation at 4°C, the cells were washed three times and then analyzed using an EPICS XL flow cytometer (Beckman Coulter).

Quantification of mRNA levels by RT-qPCR analysis

HEK293 cells were transfected with the $Nef_{NL4\text{-}3}$, $Nef_{JR\text{-}CSF}$, AA129-206-EGFP, CP-EGFP, or EGFP expression plasmid. Total RNA was extracted from these HEK293 cells using ISOGEN (Nippon Gene Co., Ltd., Tokyo, Japan) in accordance with to the manufacturer's instruction. First-strand cDNA synthesis was performed using the SuperScript™ III First-Strand Synthesis System for RT-PCR (Invitrogen, Carlsbad, CA) according to the manufacturer's instruction. DyNAmo™ HS SYBR®Green qPCR kit (FINNZYMES, Espoo, Finland) reagents were used as quantitative real-time PCR reagents according to the manufacturer's instruction. Thermocycling was carried out using the DNA Engine OPTICON®2 system (MJ Research, Inc, Waltham, MA). mRNA level was normalized to the transcript of the neomycin resistance gene, which is coded in the expression vector used. The oligonucleotide primers used for the PCR were as follows: a V5 tag sense primer, TCCTCGGTCTCGATTCTACG; a V5 tag antisense primer, TGGATCCTGGTACTCAATGGT; an EGFP sense primer, ACGTAAACGGCCACAAGTTC; an EGFP antisense primer, AAGTCGTGCTGCTTCATGTG; a NeoR sense primer, AGACAATCGGCTGCTCTGAT; and a NeoR antisense primer, AGTGACAACGTCGAGCACAG.

Results and Discussion

Detection of expression diversity of Nef proteins from small subset of HIV-1 and SIV

In the beginning of this study, we constructed expression vectors of Nef from HIV-$1_{NL4\text{-}3}$, HIV-$1_{JR\text{-}CSF}$, HIV-$1_{YU\text{-}2}$, HIV-$1_{89.6}$, and SIV_{mac239} for mammalian cells, which were appended to a V5 epitope tag at the *C*-terminal end for detection. The expression pattern of each Nef was examined at the same time. HEK293 cells transiently expressing each Nef were lysed and subjected to SDS-PAGE, followed by western blot analysis using an anti-V5 antibody, as described in Materials and Methods. As shown in Fig. 1A, the expression of each Nef variant from HIV-$1_{NL4\text{-}3}$, HIV-$1_{JR\text{-}CSF}$, HIV-$1_{YU\text{-}2}$, HIV-$1_{89.6}$, and SIV_{mac239}, were observed, in which the molecular weights of the variants were expectedly detected as 27, 29, 28, 27, and 34 kDa, respectively. Then, in spite of the fact that the same conditions in terms of the type of cell, the amount of DNA for transfection, the expression vector with the CMV promoter, and the V5 epitope for detection were used, the diversity of the expression level among the five Nef's was observed (Figure 1A). We paid attention to the heterogeneity of the expression level. We again examined the expression properties of $Nef_{NL4\text{-}3}$ and $Nef_{JR\text{-}CSF}$, respectively showing the lowest and highest expression levels, using clones of HEK293/CD4 cells stably expressing each Nef. For the expression of these proteins, the pcDNA4/HisMax vector was used, which codes for a strong translational enhancer element [30] upstream of the ATG initiation codon of Nef, and by which an increase in Nef expression level is expected. As shown in Figure 1B, the marked differences between $Nef_{NL4\text{-}3}$ and $Nef_{JR\text{-}CSF}$ were reproducibly observed among the clones tested by western blot analysis; the expression levels of $Nef_{JR\text{-}CSF}$ were more than tenfold those of $Nef_{NL4\text{-}3}$. Relatively low expression levels of $Nef_{NL4\text{-}3}$ were still observed, although the vector with the translational enhancer element was used.

We also examined the expression property by immunostaining HEK293/CD4 cells stably expressing Nef. Nef and the nucleus were respectively stained with an anti-V5 antibody and DAPI, simultaneously. Then, it was verified at a glance that all the cells expressed Nef in both clones (Figure 2). $Nef_{NL4\text{-}3}$ was predominantly detected in some of the focused areas, especially in the perinuclear region (Figure 2, top panels), which is a typical pattern of the subcellular localization of Nef [31, 32]. The regions seemed to include the *trans*-Golgi network, as previously reported [31, 32], although we have not checked for the marker by double staining. On the other hand, $Nef_{JR\text{-}CSF}$ was detected in not only the perinuclear area but also other cytosolic areas with a relatively higher fluorescence (Figure 2, bottom panels). The difference in expression level in the western blot analysis between $Nef_{JR\text{-}CSF}$ and $Nef_{NL4\text{-}3}$ (Figure 1B) was reflected in the result of the immunostaining of

Nef_{JR-CSF} and Nef_{NL4-3} (Figure 2).

Altogether, it was indicated that the extreme difference in expression level between Nef_{JR-CSF} and Nef_{NL4-3} is not due to experimental artifacts but due to the property of each Nef. Furthermore, the diversity of the Nef expression level is plausible, although more Nef clones should be examined to draw an unequivocal conclusion. Previously, Hartz et al. have reported that Nef from the HIV-1_{lai} strain shows a low expression level in COS-1 cells [33], although they have not evaluated relative expression levels among some Nef variants. At the least, a considerable difference in the level between Nef_{NL4-3} and Nef_{JR-CSF} in HEK293 cells was confirmed in these experiments.

To confirm whether both Nef_{NL4-3} and Nef_{JR-CSF} expressed in HEK293/CD4 cells are functional, their CD4 downregulation activitiy, which is the main function of Nef, were evaluated. As shown in Figure 3, the CD4 downregulation activities of Nef_{NL4-3} and Nef_{JR-CSF} were clearly observed. The activity of Nef_{NL4-3} was less than that of Nef_{JR-CSF}, in which the mean fluorescent intensities (MFIs) indicating the CD4 level in two Nef_{NL4-3}-expressing cell clones were 0.65 and 0.63, whereas those in two Nef_{JR-CSF} expressing cell clones were 0.18 and 0.12. The *N*-myristoylation at the *N*-terminus of Nef is essential for the CD4 downregulation activity [2]. To verify thether CD4 downregulation in HEK293/CD4 cells is induced by the expressed Nefs, clones of HEK293/CD4 cells expressing non-myristoylated G2A mutants of Nef_{NL4-3} or Nef_{JR-CSF} were established and the CD4 levels were evaluated. Each G2A non-myristoylated mutant of Nef_{NL4-3} or Nef_{JR-CSF} expectedly showed no CD4 downregulation. It is clear that both Nef_{NL4-3} and Nef_{JR-CSF} are certainly functional in HEK293/CD4 cells and that a high expression level of Nef is associated with efficient CD4 downregulation.

Characterization of low expression property of Nef

To determine which region of Nef_{NL4-3} is responsible for the low expression level, a chimera Nef expression vector was constructed. The primary structure of the chimera Nef tested was as follows: the first half-sequence, amino acids (AA) 1-139, was from Nef_{JR-CSF} and the second half-sequence, AA129-206, was from Nef_{NL4-3} (Figure 4A). HEK293 cells were transfected with each Nef expression vector and subjected to western blot analysis. As shown in Figure 4B, the expression level of the chimera Nef was almost the same as that of Nef_{NL4-3}. According to the quantification of the intensities of the bands with Fujifilm Image Gauge Software, the expression level of the chimera Nef was about 10% of that of Nef_{JR-CSF}. This result suggests that AA129-206 of Nef_{NL4-3}, named NLAA129-206, is required for the low expression level.

To examine whether the NLAA129-206 is not only required but also sufficient for the induction of the low protein expression level, the region was appended to the *C*- or *N*-terminal end of the enhanced green fluorescent protein (EGFP) [34, 35]. We used the combination of two protein degradation sequences, CL1 and PEST [12, 15, 36], namely, the CP sequence as a positive control of the induction of the low protein expression level. The CP sequence can induce a strong proteasome-mediated protein degradation by fusion, resulting in a low protein expression level [17, 37]. Since the PEST sequence can induce protein degradation by fusion to the *C*- or *N*-terminal end of target proteins [16], we appended the NLAA129-206 to the *C*- or *N*-terminal end of EGFP (Figures 4C). The $(GGGGS)_3$ linker was inserted between EGFP and each appended amino acid sequence (Figures 4C). It has been reported that the linker is sufficiently long and flexible to retain the function of two proteins at both ends [27]. HEK293 cells were transiently transfected with the each expression vector and cultured for 48 h. Each cellular lysate was subjected to western blot analysis as described in Materials and Methods. As shown in Figures 4D and E, the expression levels of the NLAA129-206-fused EGFPs were extremely lower than that of wild-type EGFP in the *C*- and *N*-terminal fusions. Furthermore, the expression levels of the EGFPs fused by NLAA129-206 were clearly lower than those of the EGFP fused by the CP sequence (Figures 4D and E). The β-actin levels were almost the same among the lines, showing that the amounts of loaded proteins were almost the same among the lines. Another very small band in addition to the main one was observed in EGFP (asterisk in Figure 4D), which is not identified but thought to be EGFP with posttranslational modifications. These results suggest that NLAA129-206 has a very high potential for inducing the low protein expression level by fusion. Additionally, the potential of NLAA129-206 seems to be brought out more effectively in the case of fusion to the *N*-terminal end of EGFP than in the case of fusion to the *C*-terminal end of EGFP.

To examine whether the induction of the low protein expression level by the fusion of the sequence occurs in not only EGFP but also other proteins, Rluc [29] was chosen for the experiment. Since the fusion of NLAA129-206 to the *N*-terminal end of EGFP was more effective than that to the *C*-terminal end for the induction of the low protein expression level (Figures 4D and E), the NLAA129-206 and CP sequences were appended to the *N*-terminal of Rluc for examination (Figure 4C). The expression level of Rluc could be evaluated by measuring bioluminescent activity [29]. Transiently, HEK293 cells expressing each Rluc were lysed and their Rluc activity was measured, as described in Materials and Methods. As shown in Figure 4F, the activity of NLAA129-206-fused Rluc was much lower than that of not only wild-type Rluc but also CP-fused Rluc, whose results were identical to those of EGFP (Figures 4D and E). These results suggest that the induction

of the low protein expression level by NLAA129-206 fusion universally occurs in all arbitrary proteins.

To investigate the minimum sequence of NLAA129-206 for inducing the low protein expression level, the expression levels of the three deletion mutants (NLAA142-206, NLAA129-186, and NLAA142-186) shown in Figure 5A were examined. HEK293 cells were transiently transfected with each expression vector and cultured for 48 h. Each cellular lysate was subjected to western blot analysis for EGFP fusion proteins and to the measurement of bioluminescent activity for Rluc fusion proteins, as described in Materials and Methods. As shown in Figure 5B, partial recovery of the expression levels was observed in both the N- and *C*-terminal-region-deleted mutants, namely, NLAA142-206-EGFP and NLAA129-186-EGFP, respectively. The *N*- and *C*-terminal-region-deleted mutant NLAA142-186-EGFP showed almost full recovery of its expression level, similarly to the original EGFP. Almost identical profiles of the expression pattern in Figure 5B were observed in the comparison of activity among the deletion-mutant-fused Rluc's (Figure 5C). These results suggest that the complete sequence of NLAA129-206 is required for the induction of the lowest protein expression level. It is thought that the stepwise reduction levels established by the attachment of NLAA129-206 and the mutants would become a useful repertory for inducing the desired expression of arbitrary proteins.

The NLAA129-206 regions of the Nef_{NL4-3}-corresponding sequences of Nef_{JR-CSF} and Nef_{mac239} were named JRAA139-216 and macAA161-263, respectively. The expression levels of Nef_{JR-CSF} and Nef_{mac239} were high among the five Nef's (Figure 1A). Hence, do the JRAA139-216 or macAA161-263 fusion proteins also show relatively high expression levels? The sequence-fused EGFP and Rluc (Figure 6A) expression levels were respectively examined by western blot analysis and Rluc assay. As shown in Figures 6B and C, unexpectedly, but interestingly, JRAA139-216- or macAA161-263-fused EGFP and Rluc also showed extremely low expression levels as in the cases of NLAA129-206. These results suggest that all Nef variants generally have an extremely low expression property in the *C*-terminal region. Since the chimera Nef, i.e., AA1-139 of Nef_{JR-CSF} plus NLAA129-206, showed a low expression level similarly to that of Nef_{NL4-3} (Figures 4B), it is also speculated that the contribution of AA1-139 of Nef_{JR-CSF} to the entire Nef stabilization could be restrictive to the combination of JRAA139-216.

The case with the $(GGGGS)_3$ linker resulted in a much lower expression level of EGFP by the fusion of NLAA129-206 than the case without the linker (data not shown), suggesting that the independence of NLAA129-206 from EGFP generated by the flexibility of the linker is important for the induction of the low expression level. Taking this result into consideration, JRAA139-216 might not show independence from AA1-139 of Nef_{JR-CSF} or express the potential ability to induce the low expression level, which may result in a high expression level of Nef_{JR-CSF}.

Since macAA161-263 could also induce extremely low expression levels of both EGFP and Rluc, the low expression property might be universal in Nef of not only HIV-1 but also SIV. The examination of a more comprehensive set of Nef variants might be necessary to unequivocally conclude the low expression property of the *C*-terminal region of Nef.

Examination of the mRNA levels and effect of proteasome inhibitor on the expression levels

What is the mechanism underlying the induction of the low protein expression level by the fusion of NLAA129-206? First, the mRNA level in HEK293 cells transfected with each DNA was quantified by reverse-transcription real-time quantitative PCR analysis [38]. mRNA level was normalized to the transcript of the neomycin resistance gene, which is coded in the expression vector used. Almost comparable mRNA levels between Nef_{NL4-3} and Nef_{JR-CSF}, or among EGFP, NLAA129-206 fused EGFP, and CP-fused EGFP, were observed (Figures 7A and B). These results suggest that mRNA level cannot be associated with the induction of the extremely low protein expression level.

Then, we examined protein stability. The ubiquitin proteasome system (UPS) is one of the major protein degradation machineries in eukaryotic cells [39]. Nef_{NL4-3}- or NLAA129-206-EGFP-expressing HEK293 cells were treated with the proteasome inhibitor MG132 at 20 μM for 0, 3, or 6 h. The expression level at each time point was measured by western blot analysis, which was normalized to the actin level. As shown in Figures 8A and B, increases in the apparent expression level of both proteins were slightly observed upon treatment with the inhibitor in a time-dependent manner. The results suggest that the low protein expression property of NLAA129-206 may be in part due to a high rate of protein degradation mediated by the proteasome. However, it still cannot be concluded whether the mechanism for the induction of low protein expression level is associated with protein degradation rate, since such proteasome-mediated degradation may generally occur in proteins [39]. There could be other mechanisms of inducing the low protein expression level by the *C*-terminal region of Nef. Now, we are investigating to obtain conclusive evidence from the view point of not only protein destabilization but also protein translation.

Finally, we propose that the NLAA129-206 of Nef_{NL4-3} and the corresponding regions of other Nef variants, at least from HIV-1_{JR-CSF} and SIV_{mac239}, are excellent tools for inducing extremely low expression levels of arbitrary proteins by attachment as fusion proteins. Furthermore, Nef variants from HIV and SIV viruses that are

very rich in genetic diversity may become useful resources for the search of regions inducing low protein expression levels. Such induction of extremely low protein expression levels is applicable to the development of highly responsive reporter systems [18, 19, 26], to the improvement in recombinant protein productivity [19], and to other technological research.

Acknowledgments

We thank Dr. R. Swanstrom (University of North Carolina at Chapel Hill) for helpful discussions. We thank Dr. Shinya Suzu for his kind gift of the HEK239/CD4 cells.

Funding

This study was supported in part by a Grant-in-Aid for Young Scientists from the Ministry of Education, Culture, Sports, Science and Technology of Japan and a Health and Labour Sciences Research Grant from the Ministry of Health, Labour and Welfare of Japan.

References

1. Geyer, M., Fackler, O. T. and Peterlin, B. M. (2001) EMBO Rep. **2**, 580-585
2. Fackler, O. T., Moris, A., Tibroni, N., Giese, S. I., Glass, B., Schwartz, O. and Krausslich, H. G. (2006) Virology. **351**, 322-339
3. Jere, A., Fujita, M., Adachi, A. and Nomaguchi, M. (2010) Microbes Infect. **12**, 65-70
4. Guy, B., Kieny, M.P., Riviere, Y., Le, Peuch. C, Dott, K., Girard, M., Montagnier, L., Lecocq, J.P. (1987) Nature. **330**, 266-269
5. Tebit, D. M., Nankya, I., Arts, E. J. and Gao, Y. (2007) AIDS Rev. **9**, 75-87
6. Berger, E. A., Doms, R. W., Fenyo, E. M., Korber, B. T., Littman, D. R., Moore, J. P., Sattentau, Q. J., Schuitemaker, H., Sodroski, J. and Weiss, R. A. (1998) Nature. **391**, 240
7. Taylor, B. S., Sobieszczyk, M. E., McCutchan, F. E. and Hammer, S. M. (2008) N Engl J Med. **358**, 1590-1602
8. de Sousa Abreu, R., Penalva, L. O., Marcotte, E. M. and Vogel, C. (2009) Mol Biosyst. **5**, 1512-1526
9. Lu, P., Vogel, C., Wang, R., Yao, X. and Marcotte, E. M. (2007) Nat Biotechnol. **25**, 117-124
10. Reinstein, E. and Ciechanover, A. (2006) Ann Intern Med. **145**, 676-684
11. Bachmair, A., Finley, D. and Varshavsky, A. (1986) Science. **234**, 179-186
12. Rogers, S., Wells, R. and Rechsteiner, M. (1986) Science. **234**, 364-368
13. Gilon, T., Chomsky, O. and Kulka, R. G. (1998) EMBO J. **17**, 2759-2766
14. Zhang, M., MacDonald, A. I., Hoyt, M. A. and Coffino, P. (2004) J Biol Chem. **279**, 20959-20965
15. Li, X., Zhao, X., Fang, Y., Jiang, X., Duong, T., Fan, C., Huang, C. C. and Kain, S. R. (1998) J Biol Chem. **273**, 34970-34975
16. Loetscher, P., Pratt, G., Rechsteiner, M. (1991) J Biol Chem. **266**, 11213-11220
17. Fan, F., Wood, K. V. (2007) Assay Drug Dev Technol. **5**, 127-136
18. Voon, D. C., Subrata, L. S., Baltic, S., Leu, M. P., Whiteway, J. M., Wong, A., Knight, S. A., Christiansen, F. T. and Daly, J. M. (2005) Nucleic Acids Res. **33**, e27
19. Leclerc, G. M., Boockfor, F. R., Faught, W. J. and Frawley, L. S. (2000) Biotechniques. **29**, 590-591, 594-596, 598 passim
20. Paguio, A., Stecha, P., Wood, K. V. and Fan, F. (2010) Curr Chem Genomics. **4**, 43-49
21. Ng, S. K., Wang, D. I. and Yap, M. G. (2007) Metab Eng. **9**, 304-316
22. Zubiaga, A.M., Belasco, J.G., Greenberg,M. E. (1995) Mol. Cell. Biol. **15**, 2219–2230
23. Yeilding, N. M., Rehman, M. T. Lee, W. M. (1996) Mol. Cell. Biol. **16**, 3511–3522
24. Shyu, A. B., Greenberg, M. E. and Belasco, J. G. (1989) Genes Dev. **3**, 60–72
25. Laguette, N., Benichou, S., Basmaciogullari, S. (2009) J Virol. **83**, 1093-1104
26. Takamune, N., Kuroe, T., Tanada, N., Shoji, S. and Misumi, S. (2010) Biol Pharm Bull. **33**, 2018-2023
27. Shimozono, S. and Miyawaki, A. (2008) Methods Cell Biol. **85**, 381-393
28. Takamune, N., Gota, K., Misumi, S., Tanaka, K., Okinaka, S. and Shoji, S. (2008) Microbes Infect. **10**, 143-150
29. Lorenz, W. W., McCann, R. O., Longiaru, M. and Cormier, M. J. (1991) Proc Natl Acad Sci U S A. **88**, 4438-4442
30. Stein, I., Itin, A., Einat, P., Skaliter, R., Grossman, Z. and Keshet, E. (1998) Mol Cell Biol. **18**, 3112-3119
31. Greenberg, M. E., Bronson, S., Lock, M., Neumann, M., Pavlakis, G. N. and Skowronski, J. (1997) EMBO J. **16**, 6964-6976
32. Greenberg, M. E., Iafrate, A. J. and Skowronski, J. (1998) EMBO J. **17**, 2777-2789
33. Hartz, P. A., McMiller, T., Scott-Wright, D. and Samuel, K. P. (2003) Cell Mol Biol (Noisy-le-grand). **49**,